Where in the earth are the low frequencies?: comparison of sources at Hussar

David C. Henley

ABSTRACT

Recent increased interest in full-waveform inversion of seismic reflection data has motivated attempts to broaden the spectrum of reflections recorded at the earth's surface. Of particular importance is the low frequency portion of the spectrum, which contributes significantly to the 'character' of reflections and to the ability to tie seismic data to well logs. An obvious way to boost the low-frequency spectrum is to increase the amount of low frequency source energy penetrating the earth during seismic acquisition, and to employ sensors optimized for detecting low frequencies. The objective of the Hussar experiment, performed by CREWES and some of its sponsor companies in 2011, was to test acquisition configurations designed to enhance low-frequency energy content of seismic surveys. Early results for these data compared the low-frequency spectra of the various sources on unprocessed trace gathers or on fully processed stack images. Here, in a different approach, we compare two low-frequency-optimized surface sources (Vibroseis) with buried dynamite on single source gathers from two different arrays of sensors. By separating the coherent surface-wave noise from the source gathers, we show that a larger proportion of the low-frequency source energy for the two surface sources appears as surface-wave energy, compared to dynamite. Single-fold dynamite data demonstrate both higher S/N and a broader reflection spectrum than corresponding Vibroseis data. Subsequent processing, including high-fold stacking and migration may diminish these differences, but it appears that dynamite is more effective in propagating low frequency energy into useful reflections than the surface sources tested, much of whose low-frequency output seems to preferentially excite surface waves.

INTRODUCTION

One of the ongoing challenges in exploration seismology is to produce images of the subsurface, whose traces resemble ideal well logs, accurately representing the local impedance as a function of depth. This goal is the objective of full-waveform inversion, in which algorithms are applied to reflection seismic data to broaden their spectra and extract representations of the earth's impedance function along a seismic profile. While there has been much progress in expanding the seismic spectrum on the high end, until recently, the low-frequency end was considered relatively intractable and ignored, or spliced in from existing well log information.

Recently, there has been significant effort to enhance the recovery of lower frequency information from seismic reflection data. Much of this effort has involved the use of seismic sensors, like accelerometers, with increased low-frequency sensitivity, during acquisition, as well as seismic sources designed to impart more energy into the earth in the lower frequency range. The seismic experiment conducted in the Hussar, Alberta area by CREWES and sponsors in September, 2011, investigated both of these approaches. On the source side, buried dynamite, a known low-frequency source, was compared with two surface vibrators, an INOVA 364 (specifically designed for low-frequency use), and

an Eagle Failing model y2400. Both vibrators used special sweep signals designed to spend more sweep time in the low frequency range, thus delivering more energy into the ground at those frequencies. The sweeps for both vibrators, though differing in detail, swept the frequency band from 1 to 100 Hz. Of interest to us is whether the extra source effort coupled with various low-frequency receivers significantly enhances the legitimate low-frequency content of the seismic reflections.

Earlier work has analyzed stacked, migrated sections from various combinations of sources and receivers (Isaac and Margrave, 2011), as well as single unprocessed source gathers (Margrave et al, 2011); and other work has tested the invertibility of various versions of these data (Lloyd and Margrave, 2011). The goal of the present work is to examine more closely the partition of low-frequency seismic energy into surface waves and into body waves, since only the latter contribute to actual low-frequency enhancement of reflections from subsurface interfaces. In order to do this, we examined single source gathers from a central location on the Hussar experimental line, using two different arrays of detectors, the 4.5Hz geophones, spaced 20m apart, and the Vectorseis accelerometers, spaced at 10m. We compared gathers and their spectra before and after coherent noise attenuation, as well as the 'most significant noise' component on those gathers, as estimated using radial trace techniques.

ANALYSIS METHOD

Our approach for this comparison is quite straightforward. Some previous analyses of single gathers of these data have looked at windows of raw records centred on bands of reflections, but still contaminated with coherent noise (Margrave et al, 2011). Here, we explicitly separated legitimate reflection energy from coherent noise using radial trace (RT) filtering, then analyzed spectra of raw records, filtered records, and the 'most significant' noise component, in order to show differences between the data acquired with the different sources. Since the radial trace filtering method is applied as an 'estimate and subtract' algorithm (Henley, 2003), artifacts are minimal, and coherent events remaining on gathers are primarily reflections. Hence, the gathers analyzed were roughly characterized as 'signal plus noise' (raw record), 'noise' (low-pass RT component), and 'signal' (raw record minus all 'noise' estimates).

We examined a group of source gathers on the Hussar line from source point 340 to source point 360, analyzed several, and selected one, source point 347, for which the records were good for all the data sets we used. Since the Vectorseis accelerometer array was more closely spaced than the 4.5Hz geophone array, we used the dynamite shot gather from that array to design the radial trace filters to achieve visually optimum coherent noise attenuation. The same filter parameters were then subsequently used on all the source gathers we analyzed, from both the Vectorseis array and the 4.5Hz array. The radial filter set was composed of an initial radial fan filter, followed by several pairs of radial dip filters, each aimed at a residual coherent noise of a particular apparent velocity (Henley, 2011). In every case, the initial fan filter removed the bulk of the source-generated noise, while the dip filters attenuated residual noises of relatively low amplitude, like repeated initials and their aliased events. Thus, as a reasonable estimate of the various outgoing surface waves, we displayed the noise estimate produced by the initial radial fan filter. The key to the RT filtering concept is that coherent noise which

intersects the RT fan origin (usually the shot origin on the input record) manifests only very low frequency in the radial trace domain, regardless of its native bandwidth on the original shot gather. It can subsequently be estimated by a low pass filter whose passband is well below most legitimate reflection frequencies (Henley, 2003). Since our overall goal in this work was to explore the low-frequency end of the seismic spectrum, we used Ormsby low-pass filter parameters of 1.5-2.5Hz. This means that even in the worst case of nearly vertical radial traces in the RT fan, the low-pass filters would have minimal interaction with underlying reflections. Spectra of all trace gathers in this work were computed as average spectra over all the traces in the gather, over a time window of 0-3sec, hence characterizing the entire gather.

RESULTS

4.5Hz geophone spread

We present first the results from the 4.5Hz geophone array, using source point 347. Figure 1 is an unfiltered display, with only AGC applied, of the dynamite shot from source point 347. In spite of fairly strong coherent noise, a band of reflections is easily visible between about 1000ms and 2000ms. While the coherent noise seems to consist mostly of direct arrivals and ground roll, there are also some repeated initials visible, parallel to the direct arrivals.

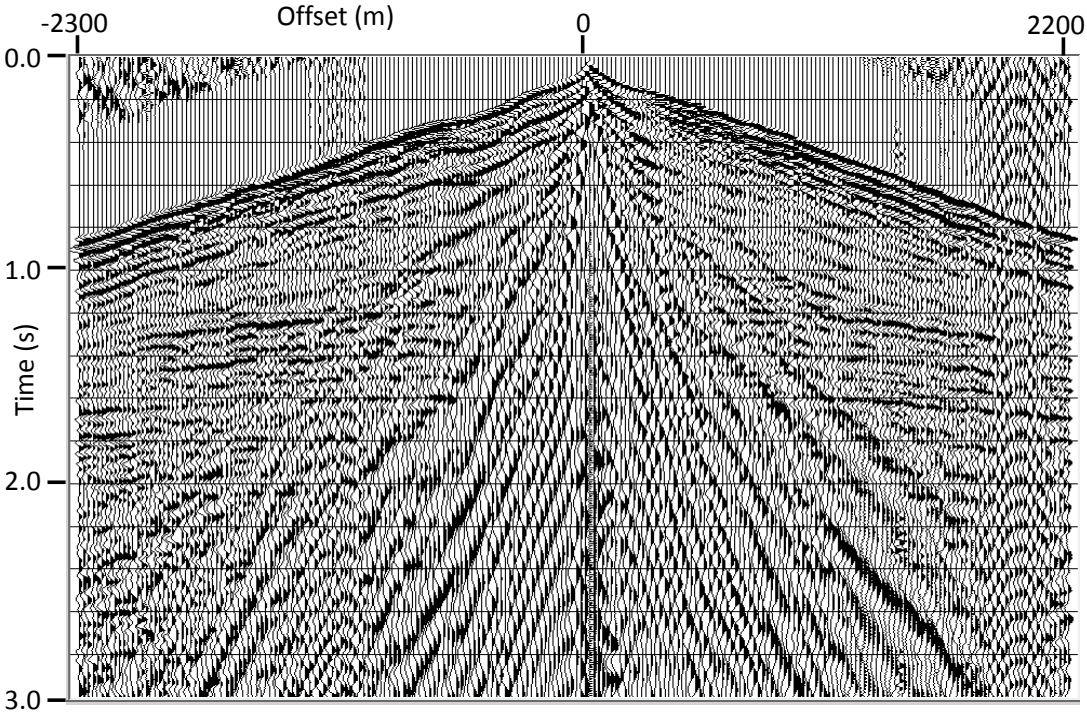

FIG.1. Dynamite source gather at source point 347 as recorded by 4.5Hz geophones. Reflections are clearly visible on this gather in spite of strong ground roll, direct arrivals, and repeated initials.

The most significant component of the coherent noise on this gather is shown in Figure 2, as estimated by the 1.5-2.5Hz low-pass filter in the radial trace (RT) domain, while Figure 3 shows the original shot gather after subtracting this component and a few relatively low-amplitude residual linear events (estimated by RT dip filters).

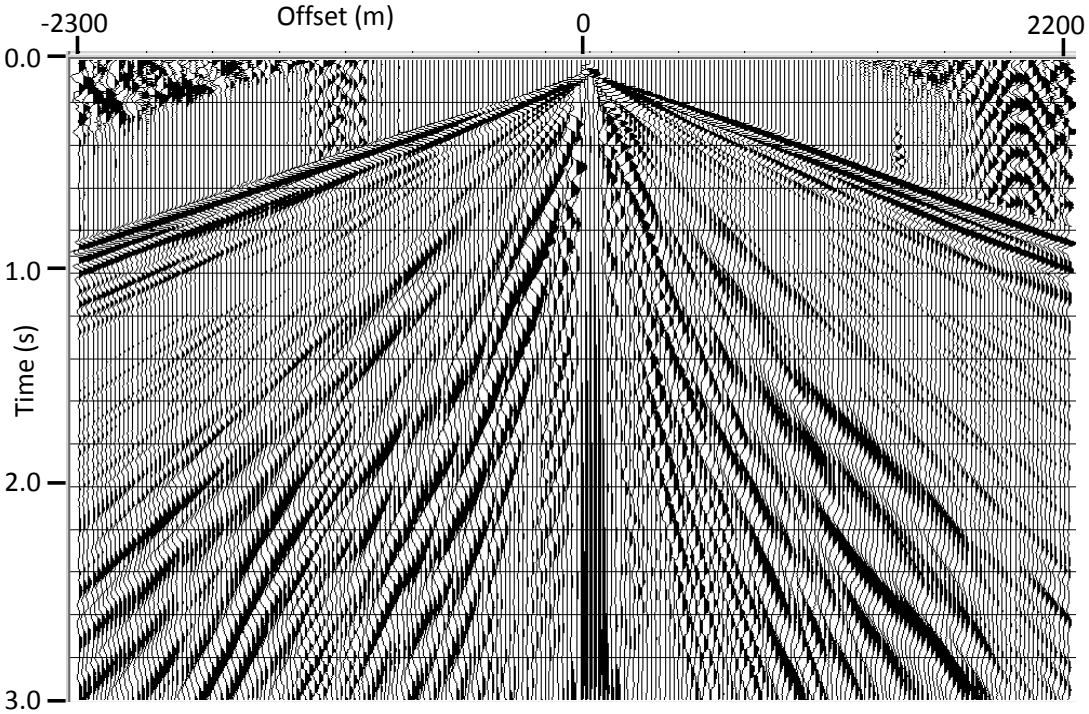

FIG.2. Most significant component of coherent noise at source point 347, as estimated in the RT domain.

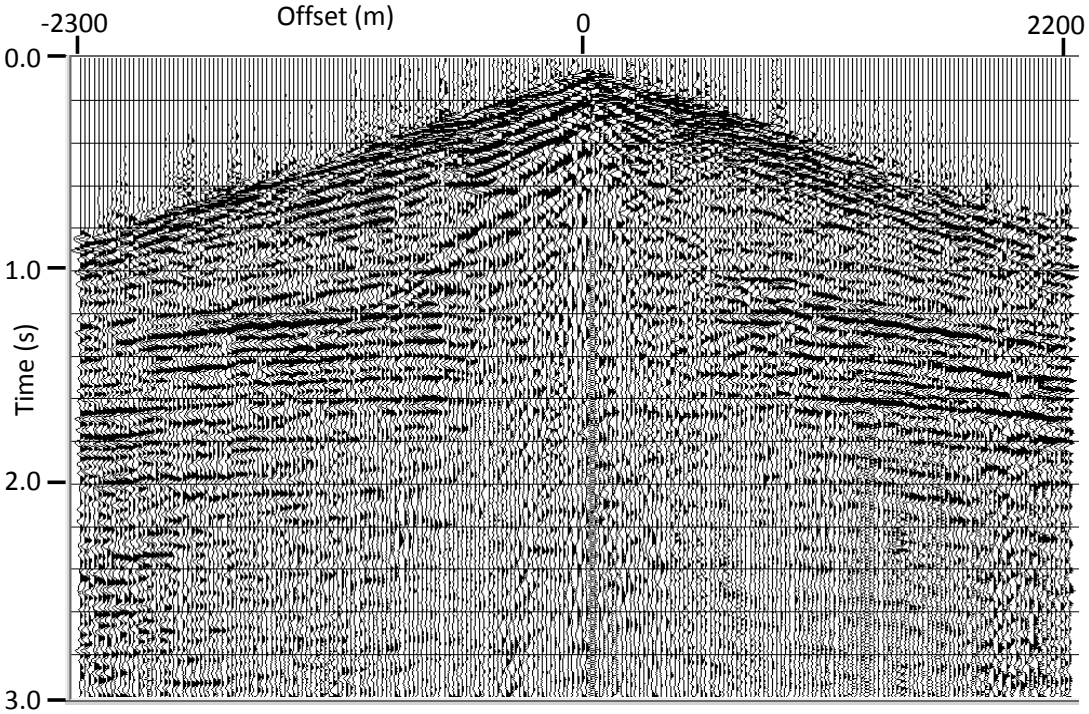

FIG.3. Dynamite source gather at source point 347 after subtraction of coherent noise estimates. Although there is some residual noise, reflections are much stronger.

Of special note in Figure 2 is the presence of some very low frequencies in the very near offset traces. Figure 4 presents the power spectrum of the 0-3000ms raw shot record, averaged over all traces, Figure 5 shows the spectrum of the noise estimate in Figure 2, and Figure 6 is the spectrum of the shot record minus the coherent noise. Next we look at the low-frequency portions of these spectra more closely in Figures 7, 8, and 9. The spectrum of the raw shot, in Figure 7, exhibits considerable power as low as 4Hz, and declines by only 6dB at 3Hz, while on the upper end, the slope of the spectrum declines from full strength at 20Hz to -6dB at 24Hz. The question is, what portion of the spectrum is attributable to reflection energy, and what portion to coherent noise? The low-frequency detail spectrum in Figure 8 demonstrates that the coherent noise energy peaks at 4Hz, but exhibits some power throughout the seismic band. The spectrum of the shot after noise removal, in Figure 9, however, demonstrates that the predominant frequency of the reflections is around 20Hz, with a lower, broader peak at 10Hz, and that most of the low-frequency energy, centred on 4Hz on the raw shot gather is contributed by the surface wave noise. If we assume that the spectrum in Figure 9 characterizes the reflections visible in Figure 3, we note that the low-frequency spectrum declines by about 14dB from 10Hz down to 2Hz.

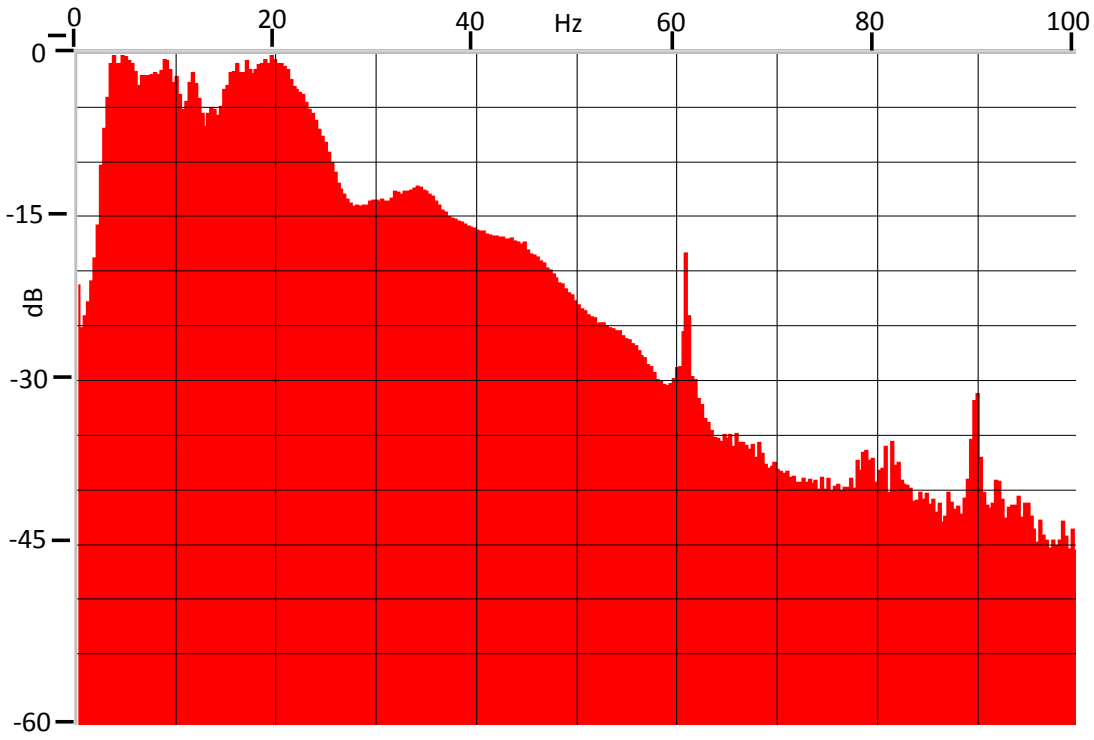

FIG.4. Power spectrum of the raw dynamite shot gather in Figure 1

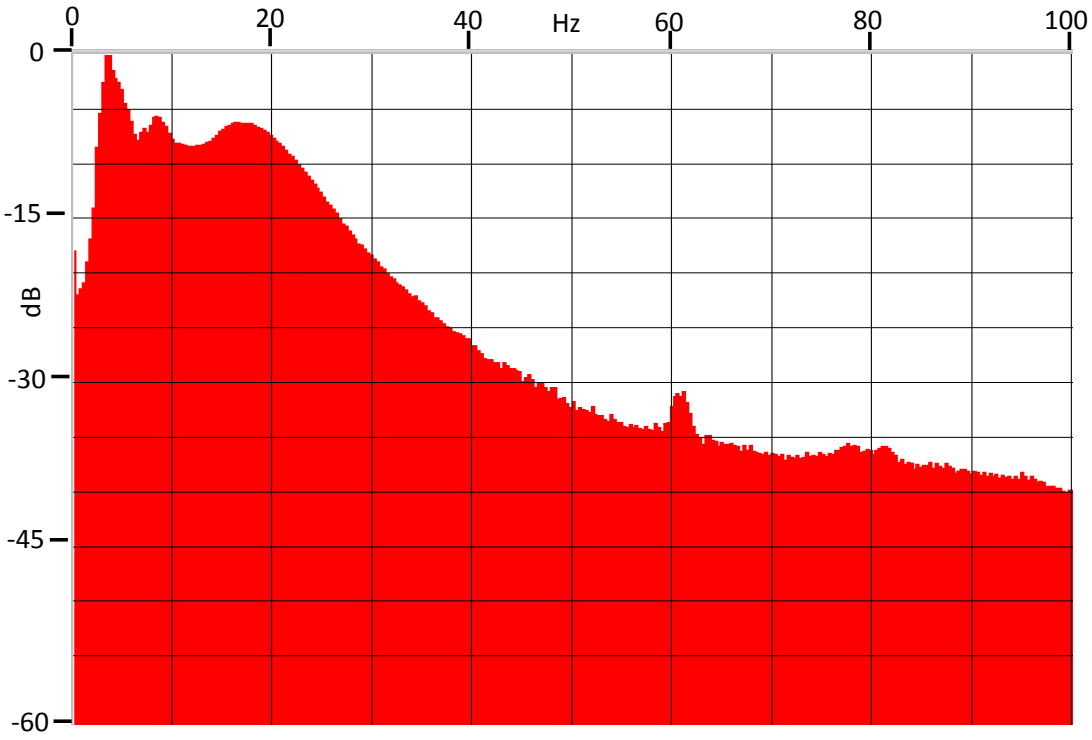

FIG.5. Power spectrum of the coherent noise estimate in Figure 2.

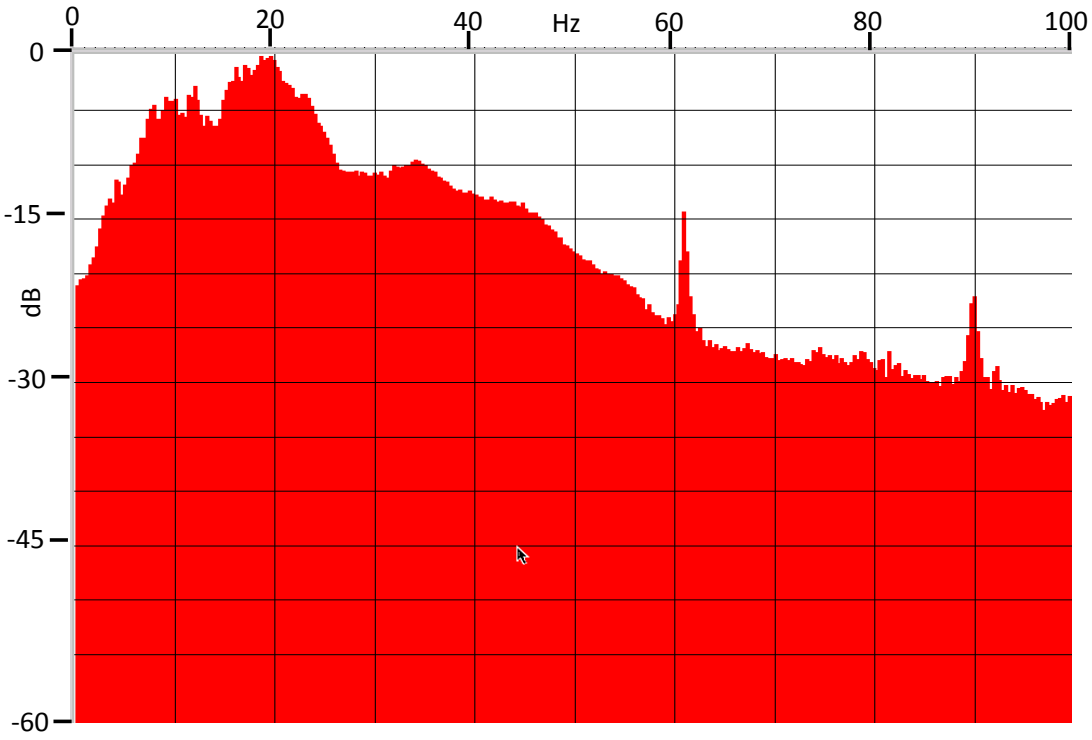

FIG.6. Power spectrum of dynamite shot gather after subtraction of coherent noise.

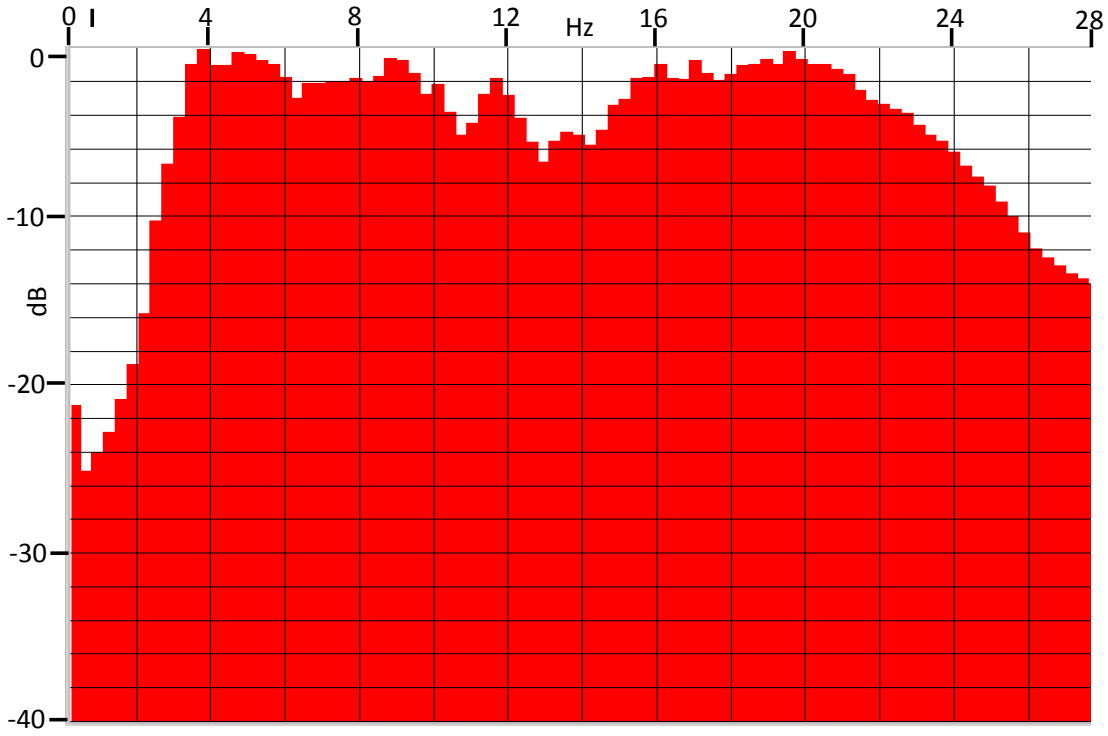

FIG.7. Low-frequency detail of spectrum in Figure 4—raw dynamite shot.

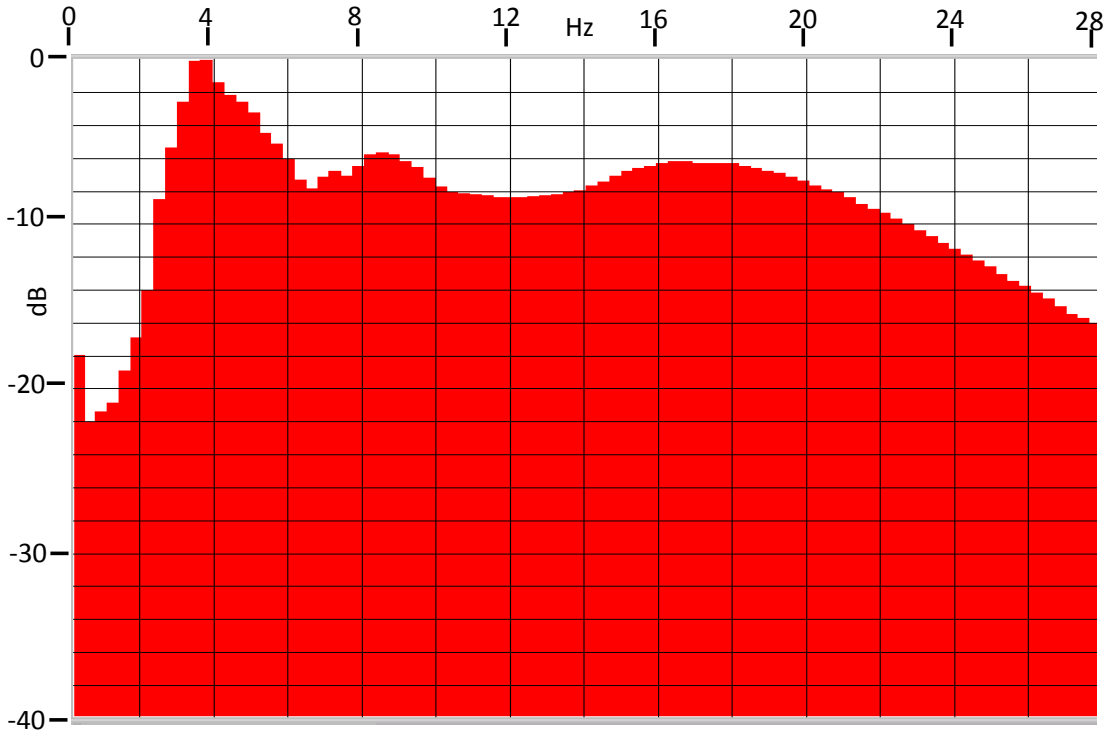

FIG.8. Low-frequency detail of spectrum in Figure 5—coherent noise estimate.

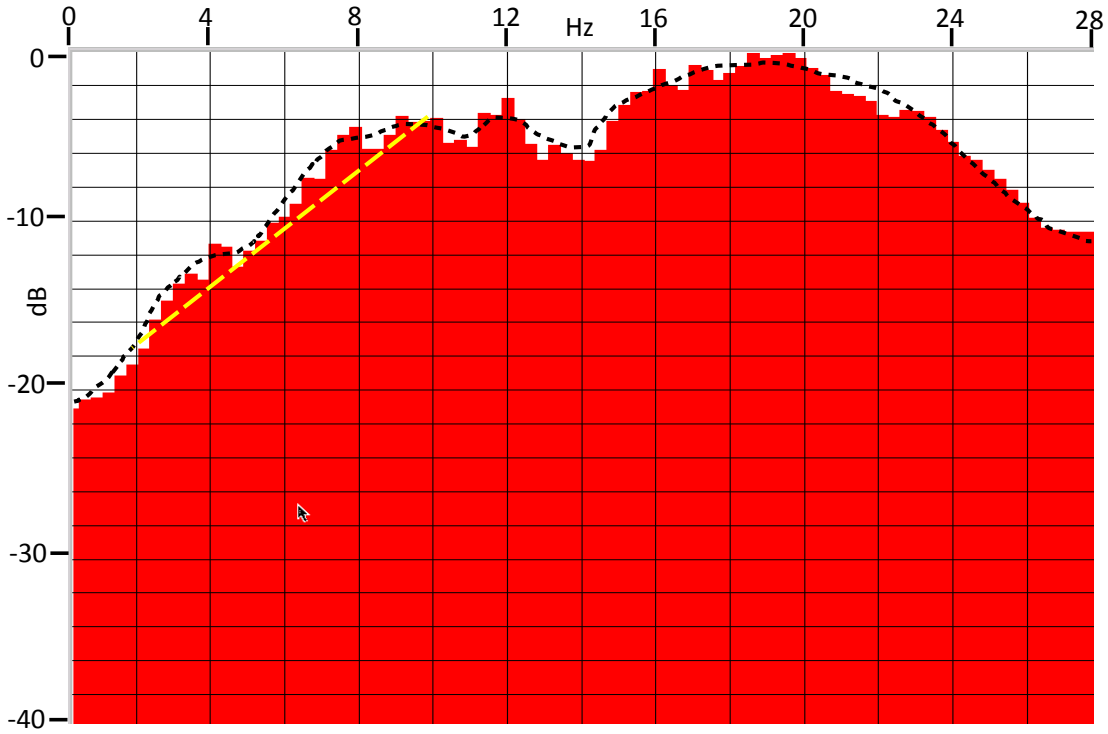

FIG.9. Low-frequency detail of spectrum in Figure 6—shot minus coherent noise. Smoothed spectrum is dotted outline, approximate low-frequency roll-off marked by dashed yellow, from 10Hz down to 2Hz.

Looking next at the source gather from the Eagle Failing y2400 vibrator at the same source point, the raw data are presented in Figure 10, the coherent noise estimate in Figure 11, and the gather after noise removal in Figure 12. It is immediately evident that, in comparison with the dynamite shot in Figure 1, reflections are visibly much weaker, relative to the coherent noise. The coherent noise estimate in Figure 11 looks similar to that in Figure 2 for dynamite, but appears deficient in the very low frequencies seen in the centre of the record in Figure 2, possibly an indication that the vibrator simply doesn't put much energy into the ground at these very low frequencies. Even after coherent noise attenuation using the same filter parameters as for the dynamite data, the reflections on the filtered trace gather in Figure 12 are not as strong, and there appears to be a higher level of residual coherent and random noise than on the gather in Figure 3. The low-frequency spectrum of the raw shot in Figure 10 is shown in Figure 13. As with the dynamite raw shot spectrum in Figure 7, a peak appears at 4Hz, but the spectrum begins its high frequency roll-off at around 16Hz, rather than the 20Hz seen on the dynamite data. Furthermore, the 4Hz peak has more amplitude than the 16Hz component, whereas on the dynamite data, the 20Hz component is comparable in strength to the 4Hz peak. The spectrum of the noise estimate, in Figure 14, exhibits the same strong peak at 4Hz as seen in the dynamite data (Figure 8), but has less power both at higher frequencies and very low frequencies (below 1Hz.) After coherent noise subtraction, the power spectrum exhibits a broad peak at around 14Hz, but shows the same -14dB decline between 10Hz and 2Hz (Figure 15). Thus the filtered gather in Figure 12 has a lower dominant

frequency, but about the same low-frequency spectrum as dynamite data. Nevertheless, the S/N is visibly lower on this record.

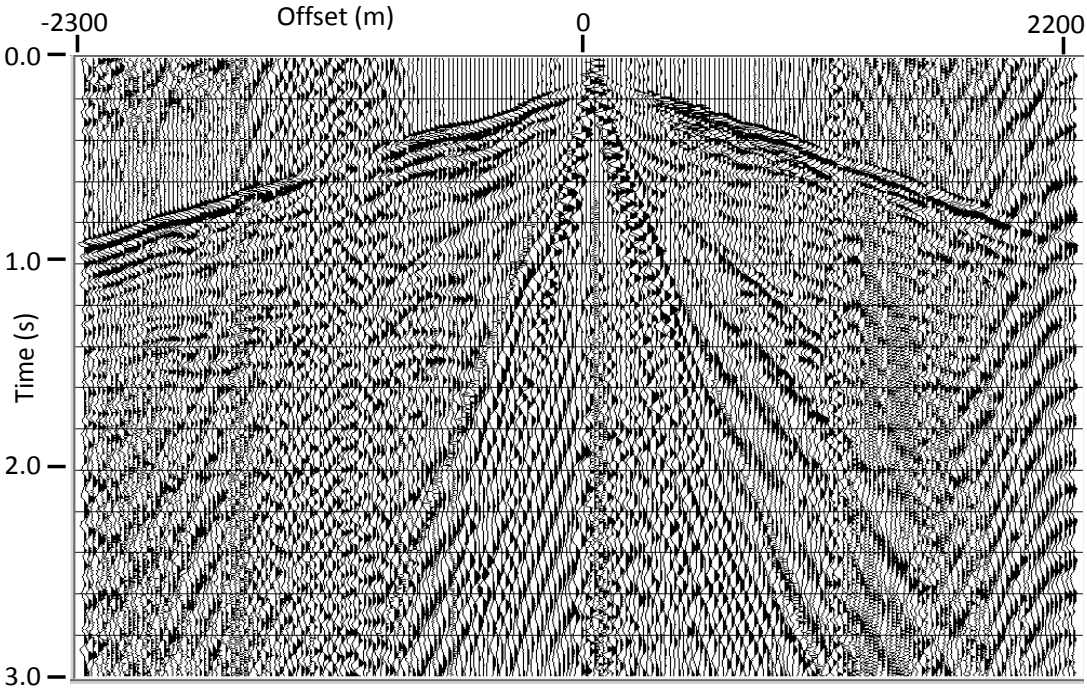

FIG.10. Source gather for the EagleFailing y2400 vibrator at source point 347 on the 4.5Hz geophone spread. Reflections are much weaker relative to coherent noise and stationary noise on this gather than on the dynamite shot gather in Figure 1.

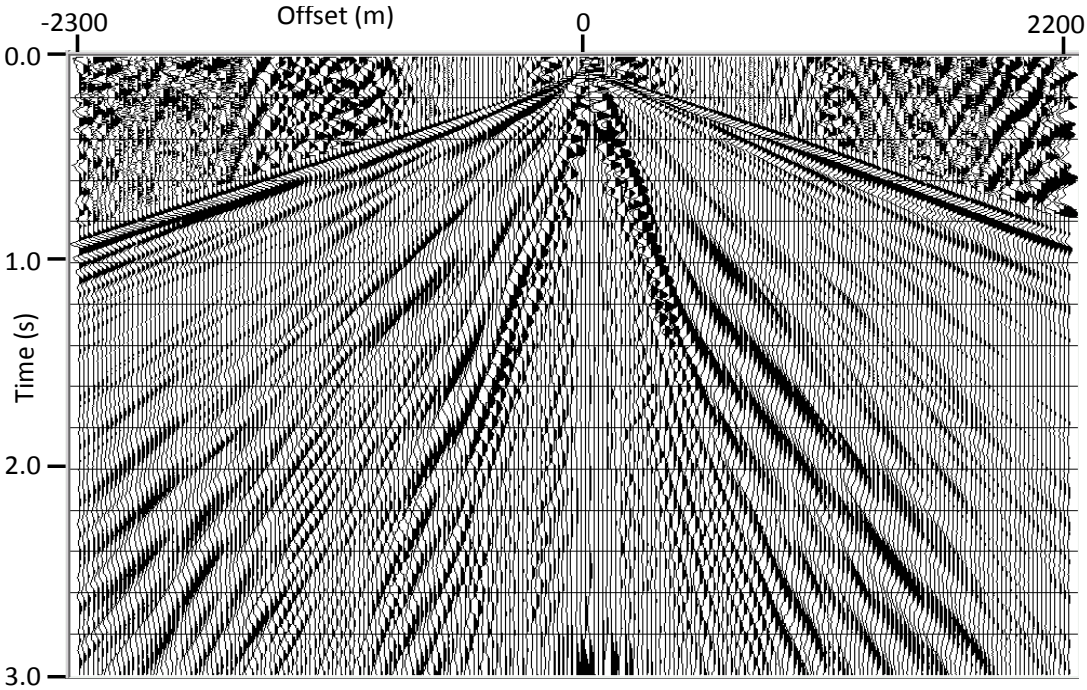

FIG.11. Most significant component of coherent noise in Source gather in Figure 10, as estimated in the RT domain.

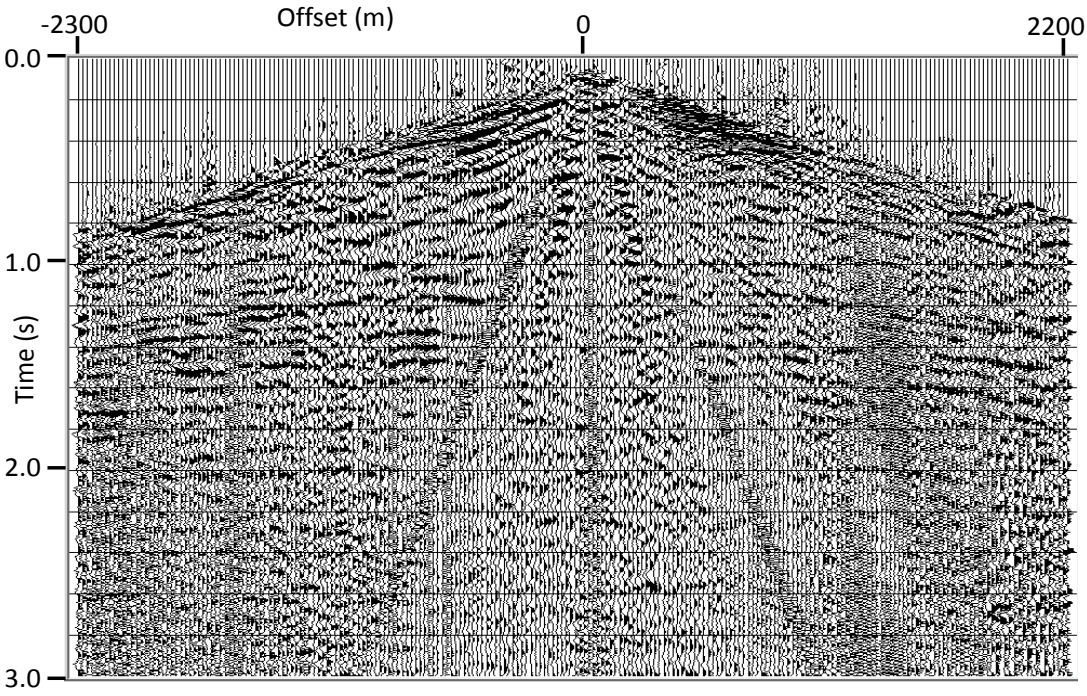

FIG.12. y2400 source gather from Figure 10 after subtraction of coherent noise estimates.

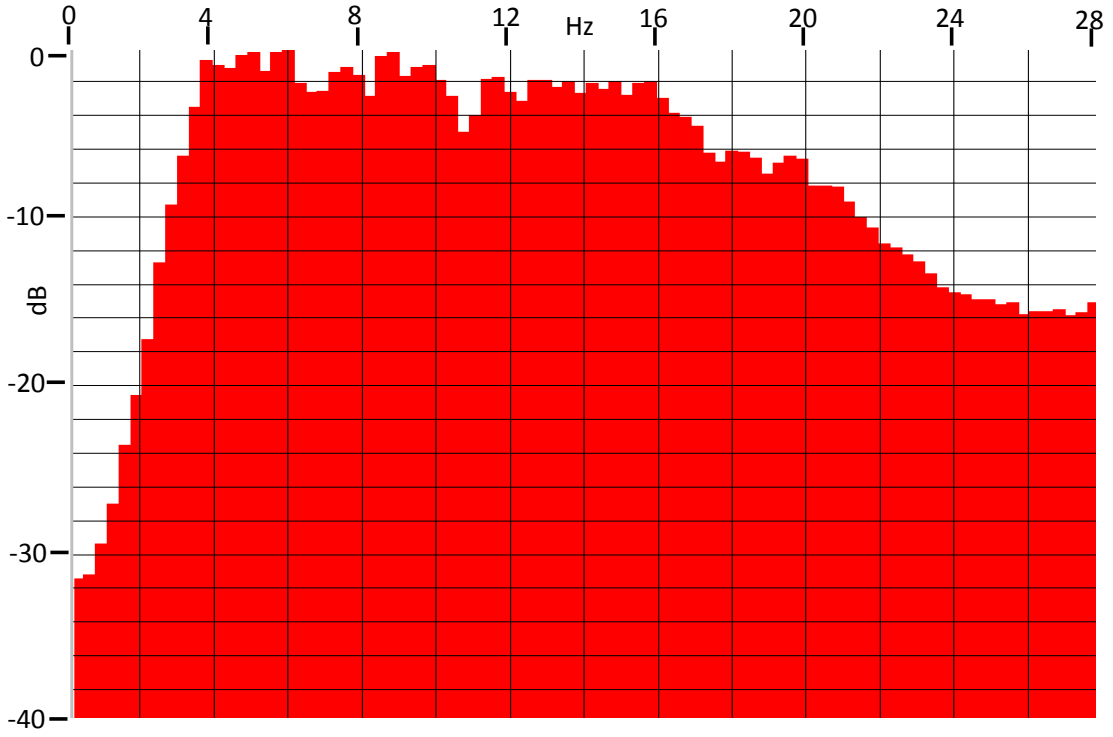

FIG.13. Low-frequency spectrum of raw source gather in Figure 10.

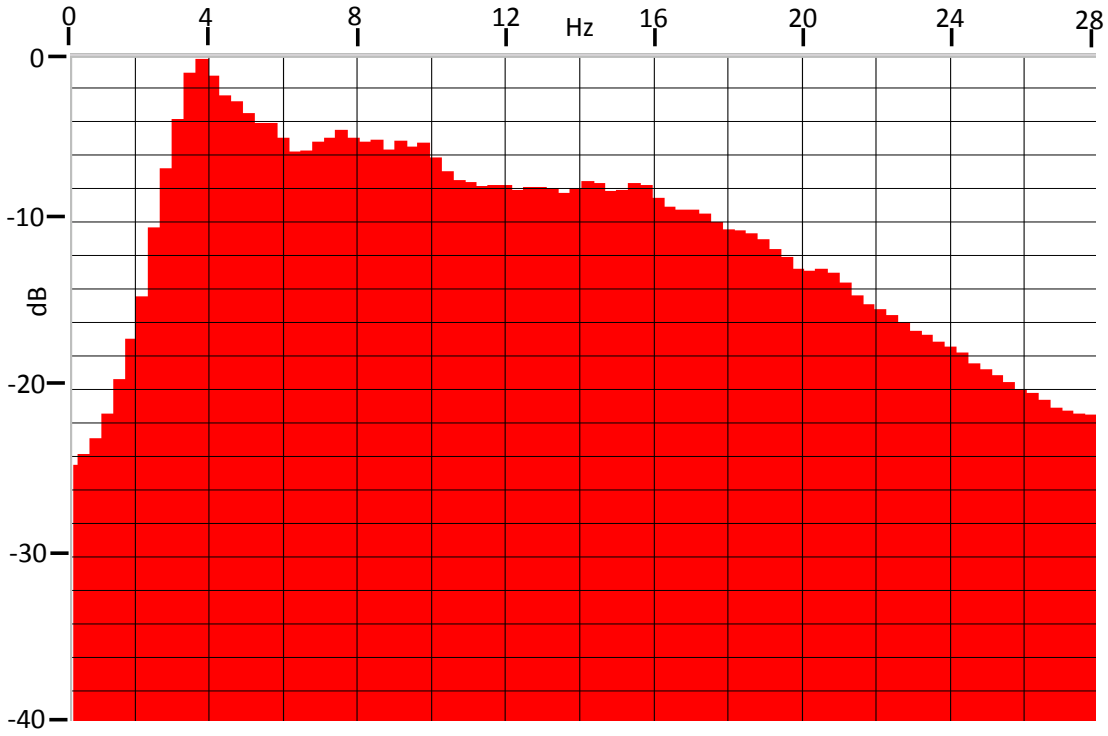

FIG.14. Low-frequency spectrum of coherent noise estimate in Figure 11.

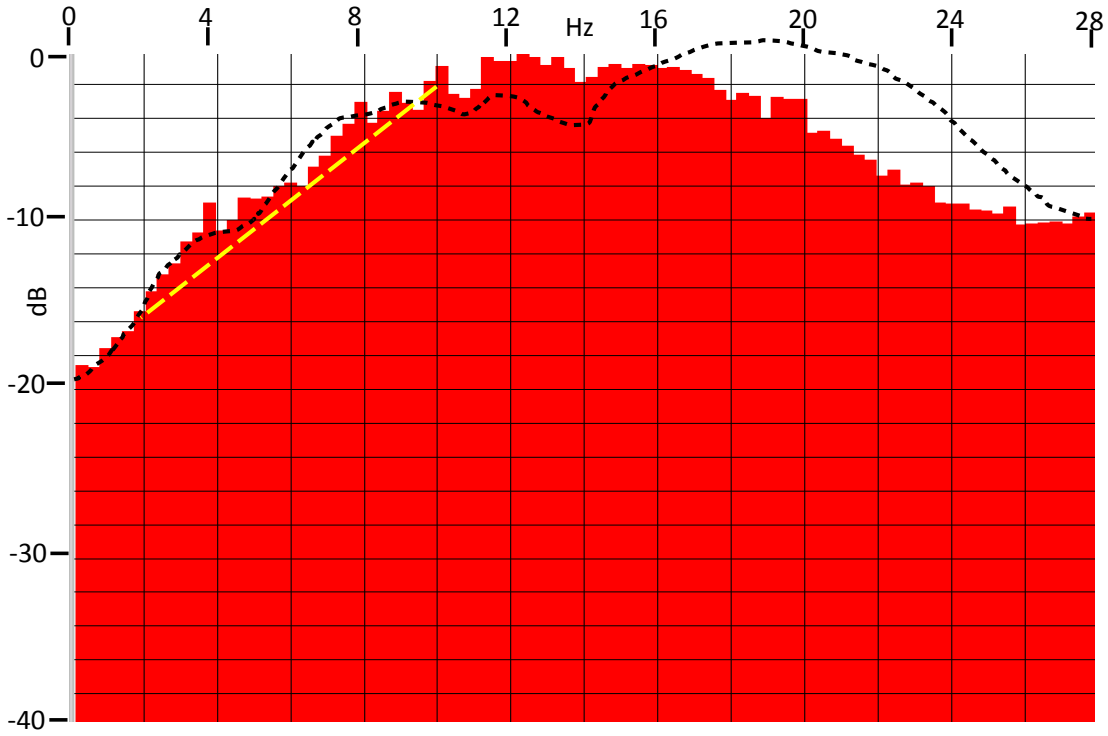

FIG.15. Low-frequency spectrum of y2400 source gather after subtraction of coherent noise. Dynamite spectrum superimposed for comparison, 2Hz-10Hz slope the same as in Figure 9.

The raw source record for the INOVA 364 vibrator, in Figure 16, looks very similar to that for the Eagle Failing vibrator (Figure 10)—low reflection visibility and an abundance of noise. The coherent noise estimate in Figure 17 is likewise similar to that in Figure 11, as is the noise-attenuated source gather in Figure 18, except that the reflections seem somewhat stronger on the INOVA record (compare with Figure 12). Comparing the low frequency spectra of the INOVA raw shot, noise estimate, and noise-attenuated shot, Figures 19, 20, and 21, respectively, with the corresponding spectra for the Eagle Failing vibrator (Figures 13, 14, and 15) reveals few significant differences. The low-frequency spectrum of the gather after noise subtraction once again shows a decline of about 14dB between 10Hz and 2Hz, and a dominant frequency of around 14Hz. The low-frequency spectrum of the Eagle Failing vibrator (Figure 15) appears somewhat smoother than that of the INOVA vibrator (Figure 21), which correlates with the somewhat lower visibility of the reflections on these data. The similarity of the low-frequency spectral slope for all three sources may reflect the intrinsic geophone response, rather than any inherent source characteristic, since no attempt was made to compensate for the phone response on any of the data sets.

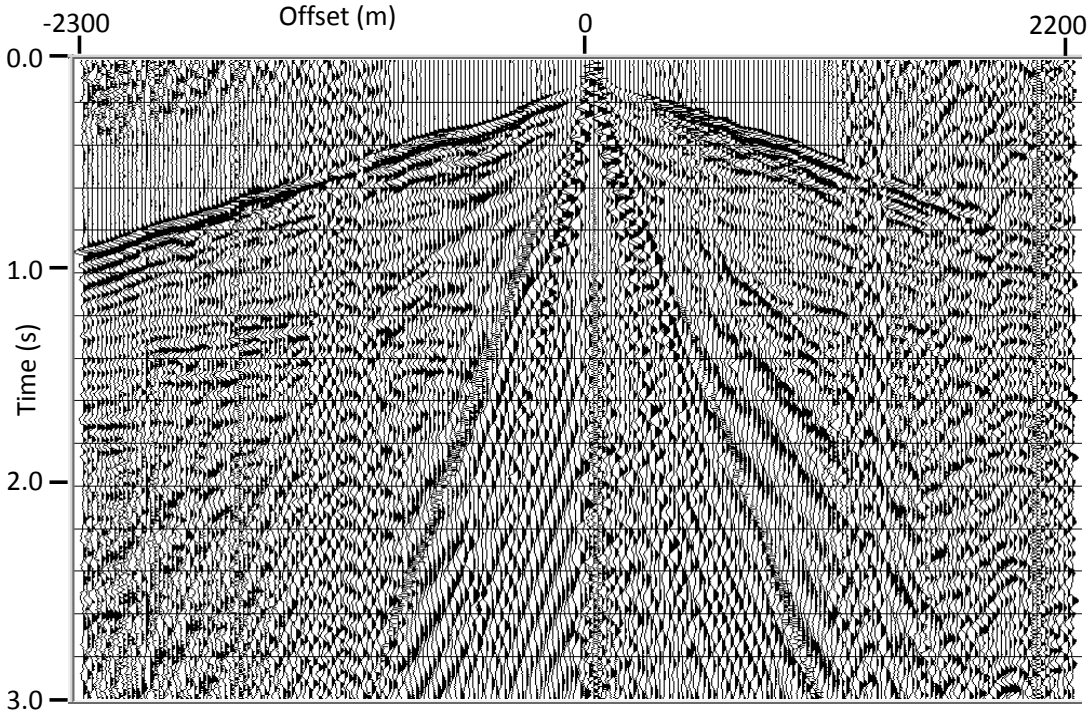

FIG.16. Source gather for INOVA Low-dwell vibrator at source point 347 on 4.5Hz geophone spread. Like the source gather in Figure 10, reflections are weaker relative to both stationary and coherent noise than on the comparable dynamite source gather in Figure 1.

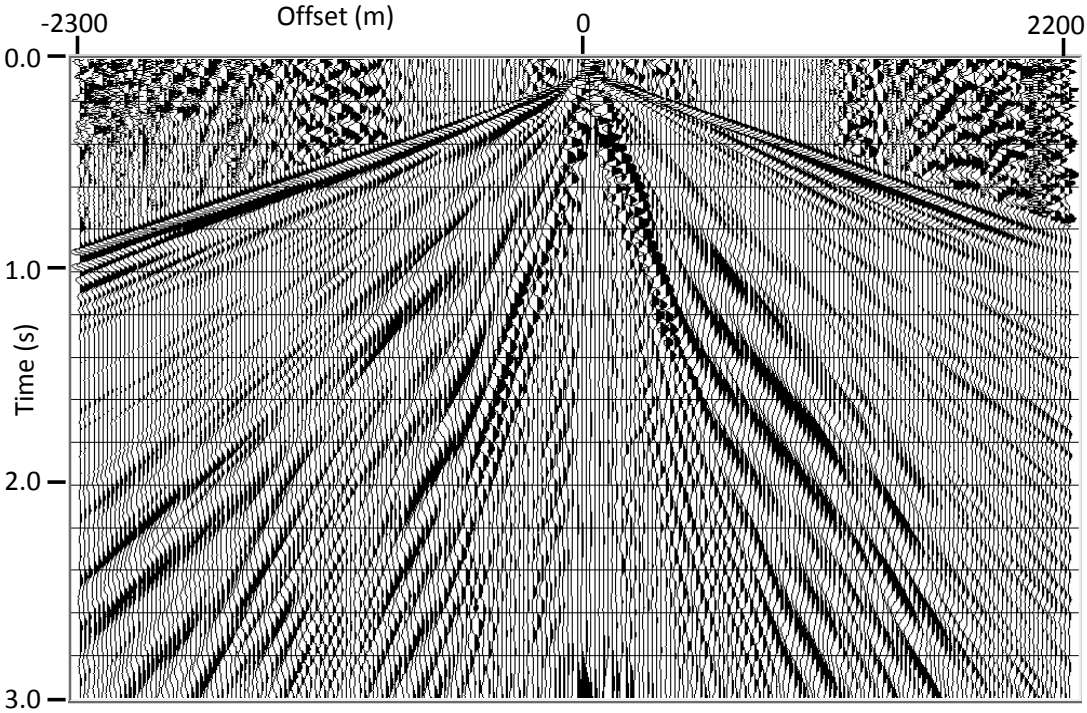

FIG.17. Most significant component of coherent noise for source gather in Figure 16, as estimated in the RT domain.

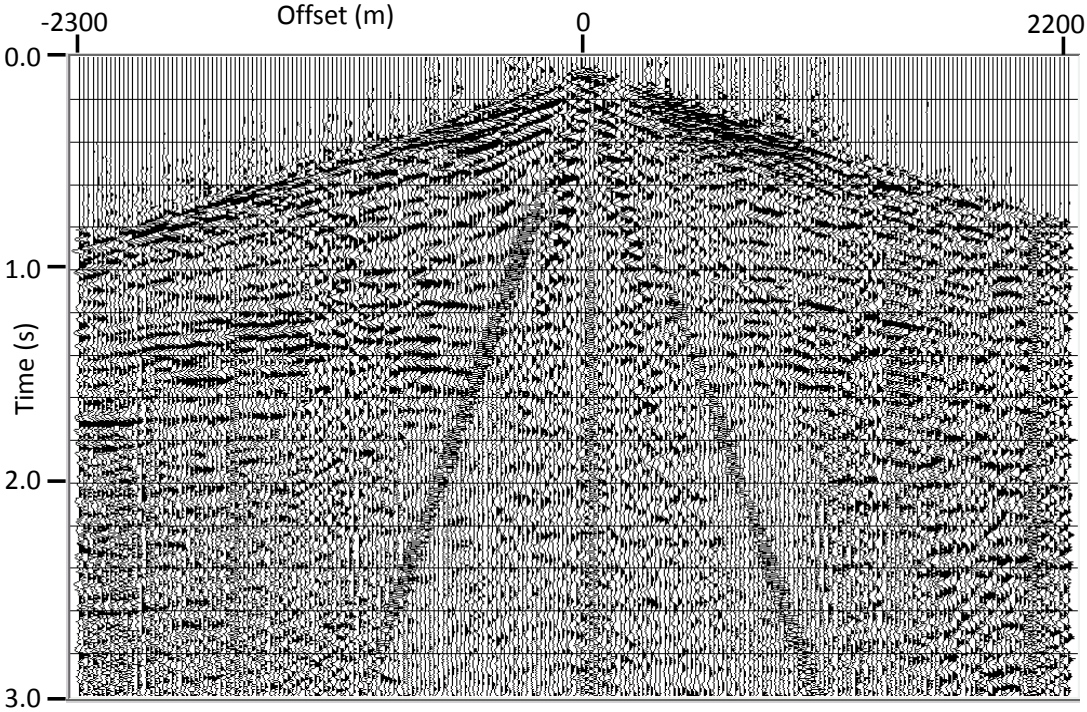

FIG.18. INOVA source gather after subtraction of coherent noise estimates.

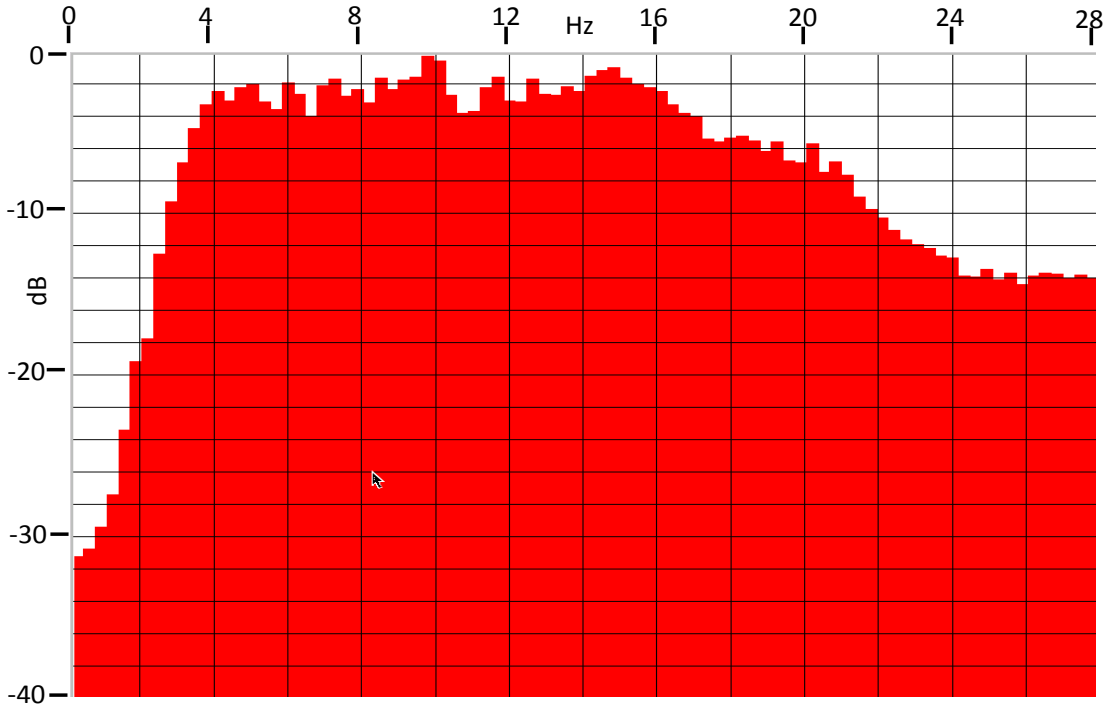

FIG.19. Low-frequency spectrum of INOVA raw source gather in Figure 16.

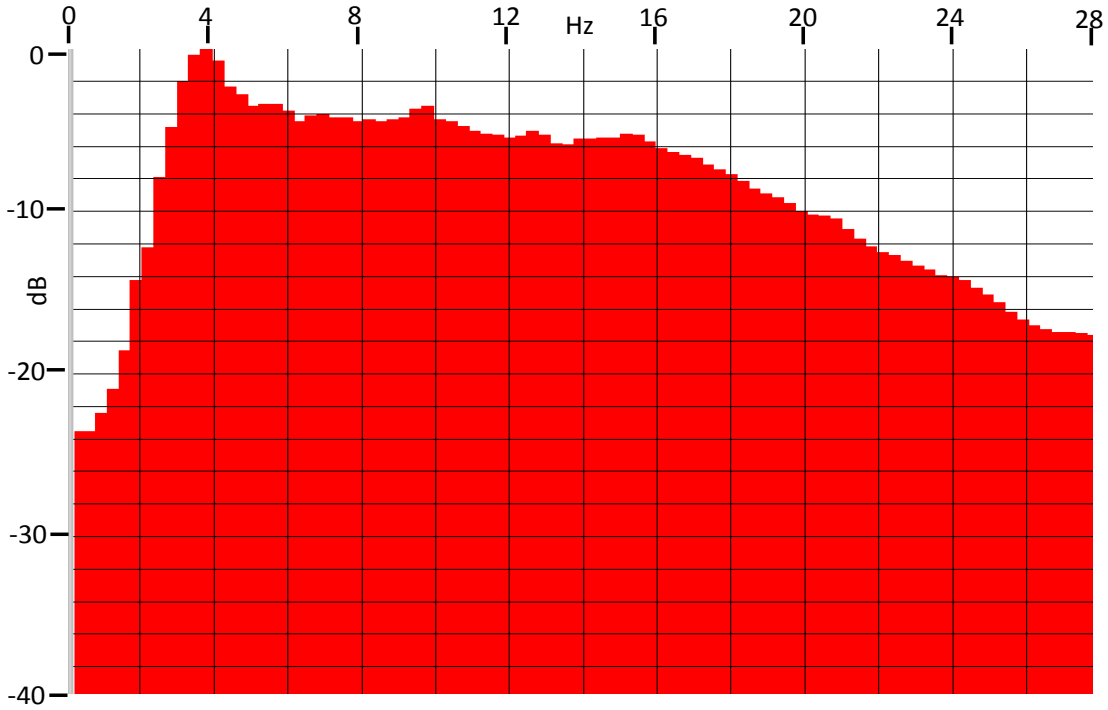

FIG.20. Low-frequency spectrum of coherent noise estimate in Figure 17.

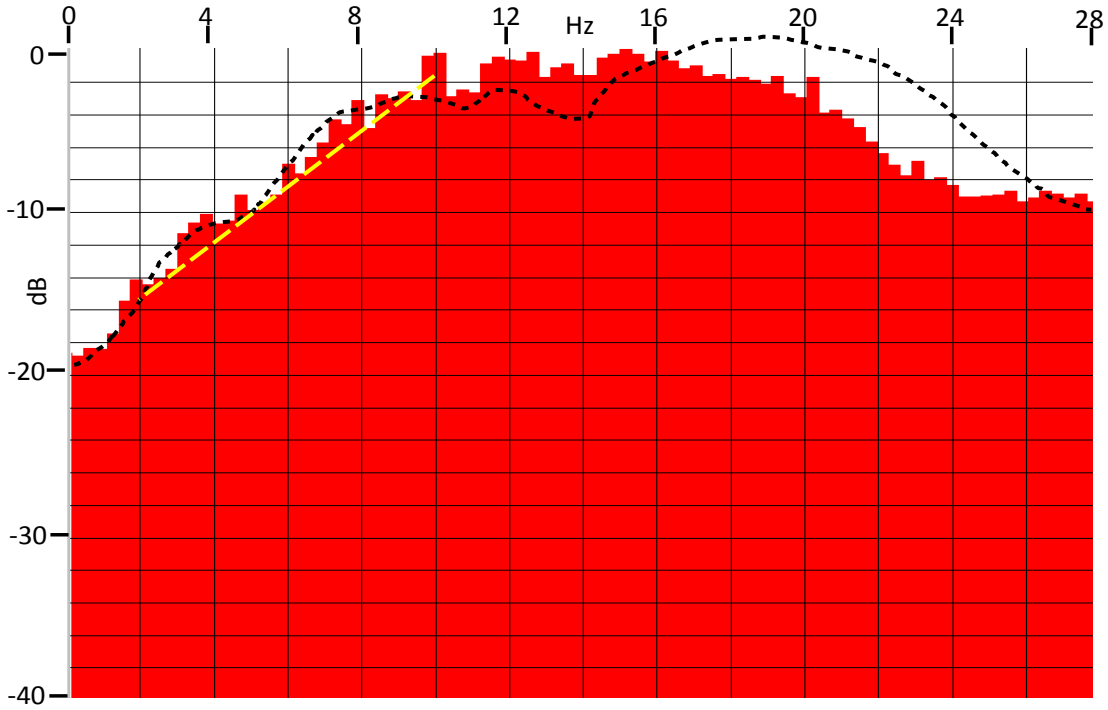

FIG.21. Low-frequency spectrum of INOVA source gather after subtraction of coherent noise. Dynamite spectrum superimposed for comparison. 2Hz-10Hz slope same as Figure 9.

Vectorseis accelerometer spread

Because the sensor spacing of the Vectorseis sensors was only half that of the 4.5Hz geophones, the source gathers displayed significantly less aliasing of noise events, making it easier to separate coherent noise. In fact, on data recorded with this spread, we were able to detect and remove a low-velocity aliased event which was unseen on the 4.5Hz data. On the other hand, the data must be integrated, which inevitably induces some low-frequency 'drift', particularly visible on raw, unfiltered records. This drift appears as trace-to-trace amplitude fluctuations on the dynamite shot gather displayed in Figure 22. The coherent noise estimate for this shot is shown in Figure 23, and the filtered shot record in Figure 24. Note that the low-frequency trace amplitude fluctuations persist on this gather, even after most of the coherent noise is successfully removed. On the low-frequency spectrum of the raw shot gather (Figure 25), in addition to the 4Hz peak corresponding to coherent noise, we note a peak just below 1Hz, which is the likely signature of this integration-induced 'drift'. The spectrum of the noise estimate, in Figure 26, captures both the 4Hz coherent noise peak and the very strong 'drift' peak. Nevertheless, even after subtracting the noise estimate, some of the 'drift' component remains in the data (Figure 24). The small peak at 4Hz on the low-frequency spectrum of the shot after filtering (Figure 27), on the other hand, may actually be part of the reflection spectra, as recorded by Vectorseis accelerometers. Looking again at Figure 24, we can see what may be some of this lower-frequency energy later in the record in the centre of the spread; and it is laterally coherent, in contrast to the 'drift' fluctuations.

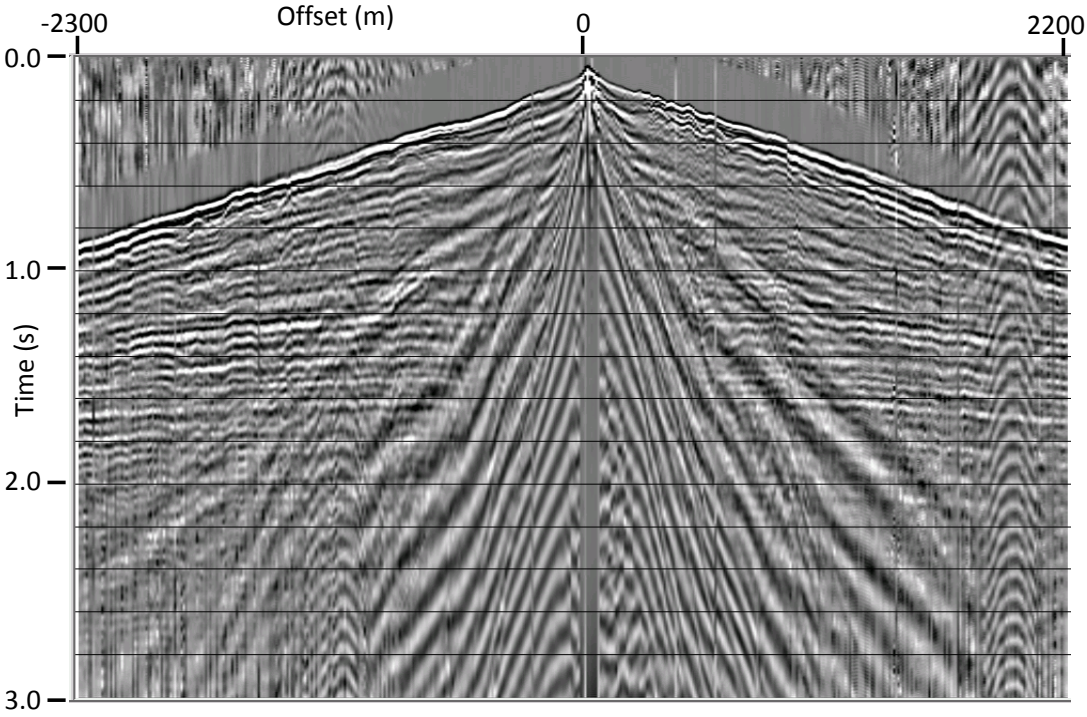

FIG.22. Dynamite vertical component source gather at source point 347 as recorded by the Vectorseis accelerometer spread. Reflections are easily visible.

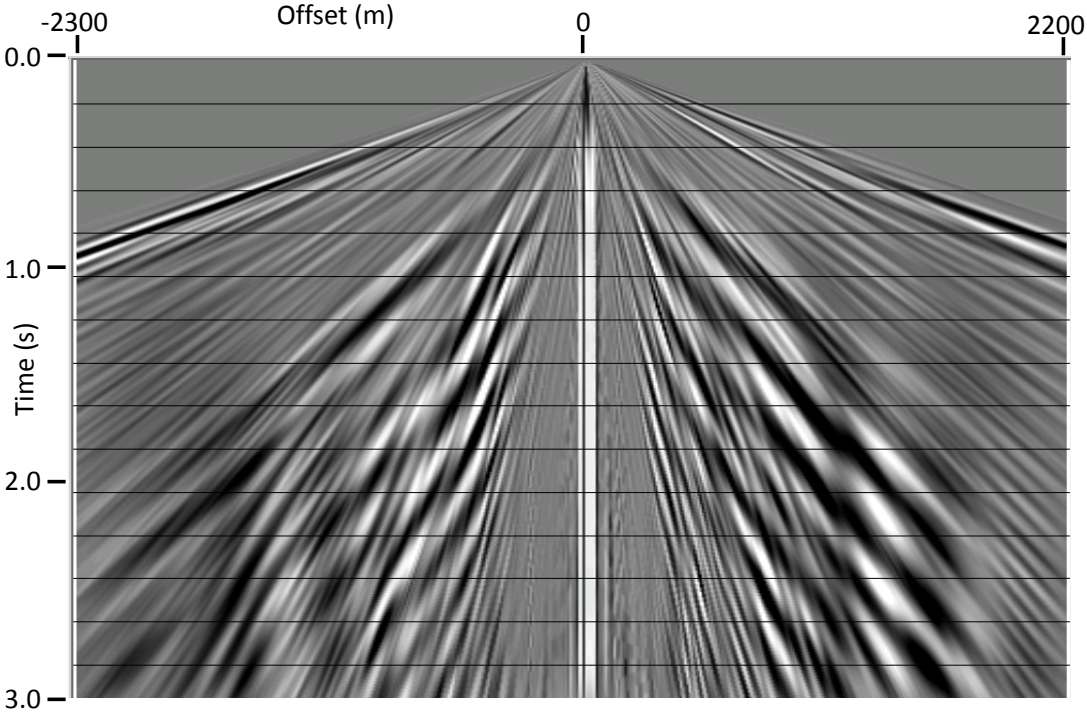

FIG.23. Most significant coherent noise component as estimated in the RT domain.

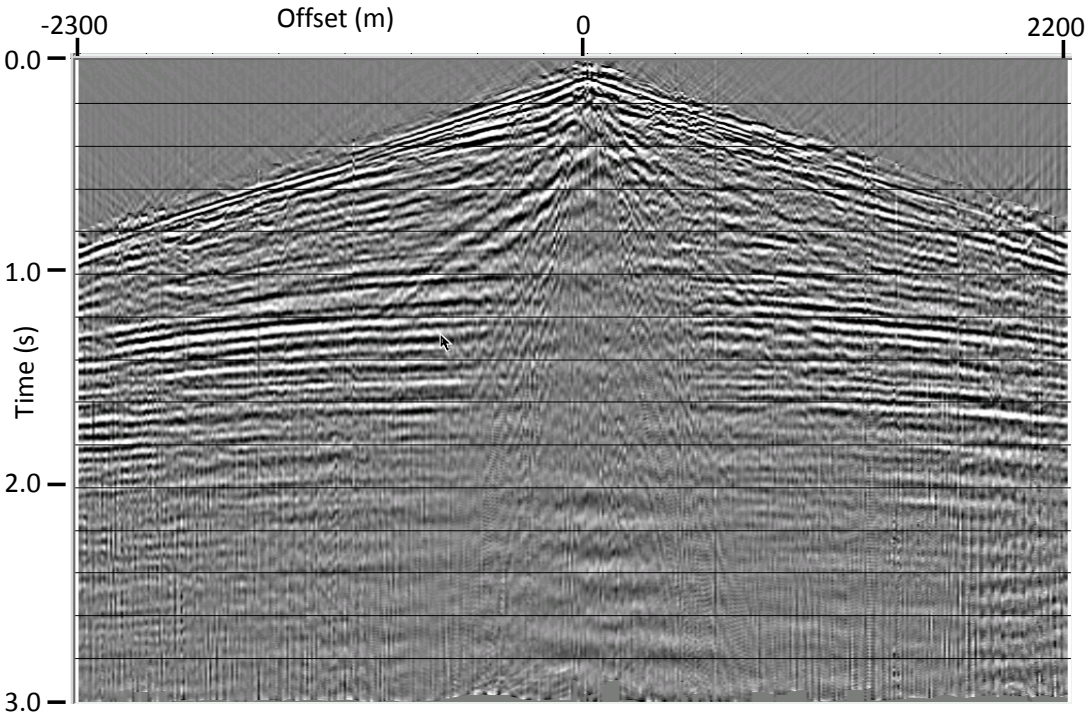

FIG.24. Dynamite source gather after subtraction of coherent noise estimates.

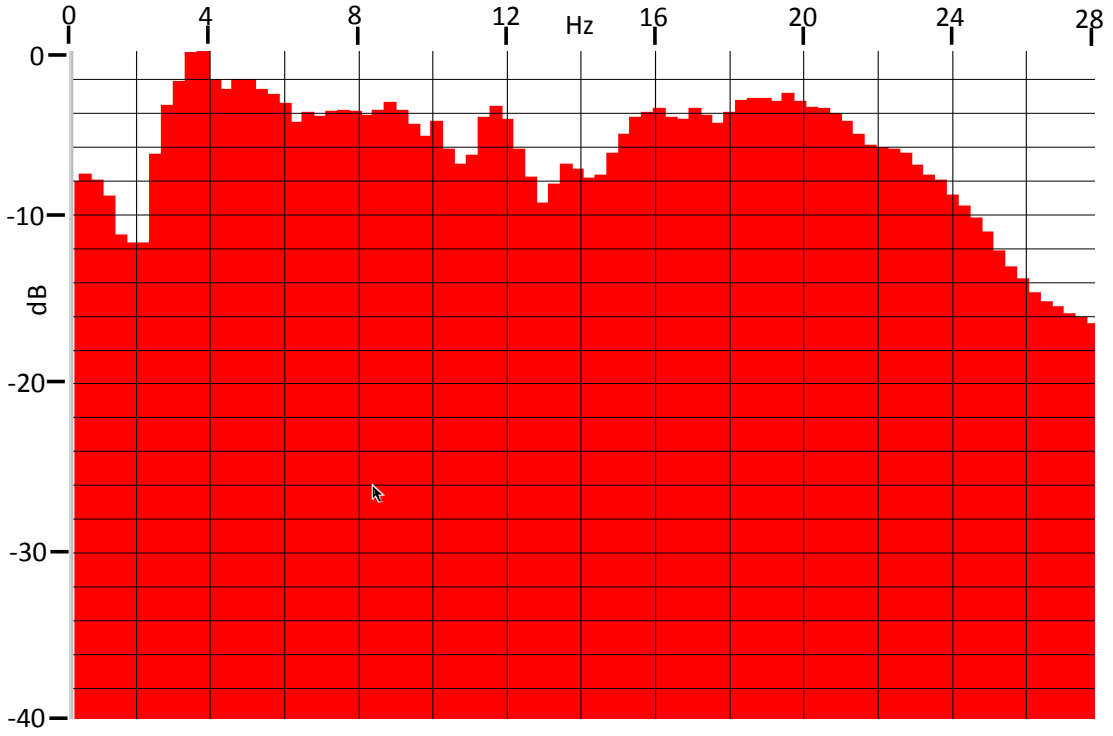

FIG.25. Low-frequency spectrum of Dynamite source gather in Figure 24. Power in the spectrum below 2Hz is likely due to integration 'drift' for accelerometers.

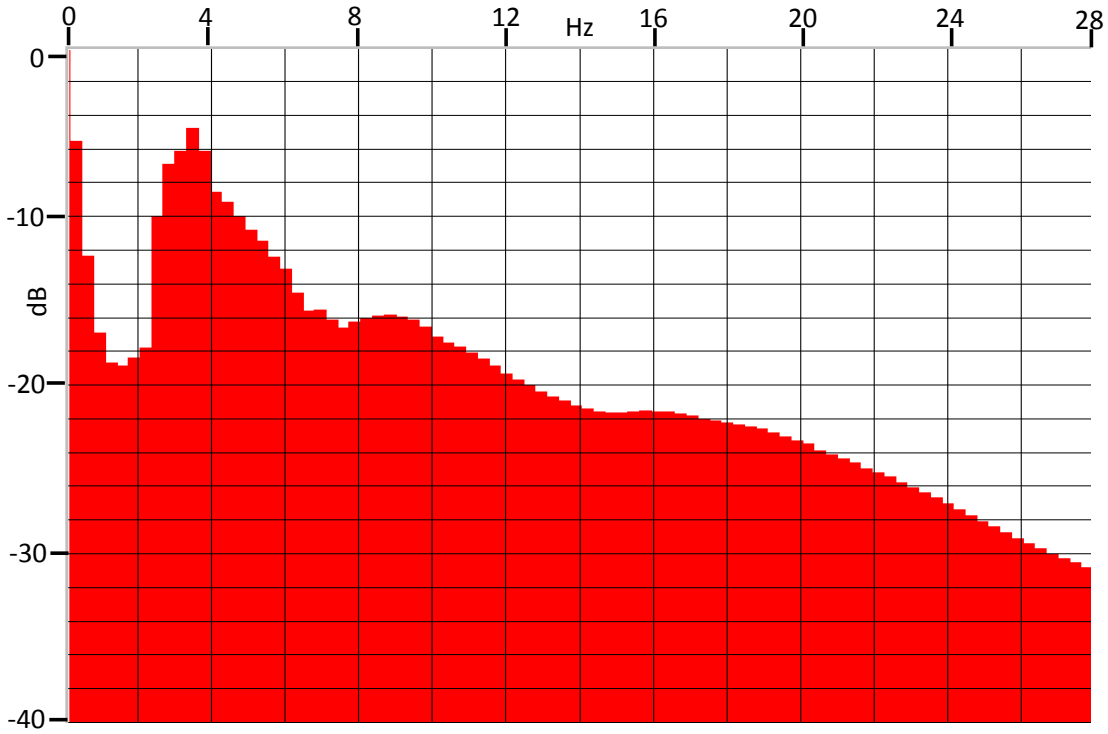

FIG.26. Low-frequency spectrum of coherent noise estimate in Figure 23. Power below 2Hz is likely 'drift' introduced by integration of accelerometer signals.

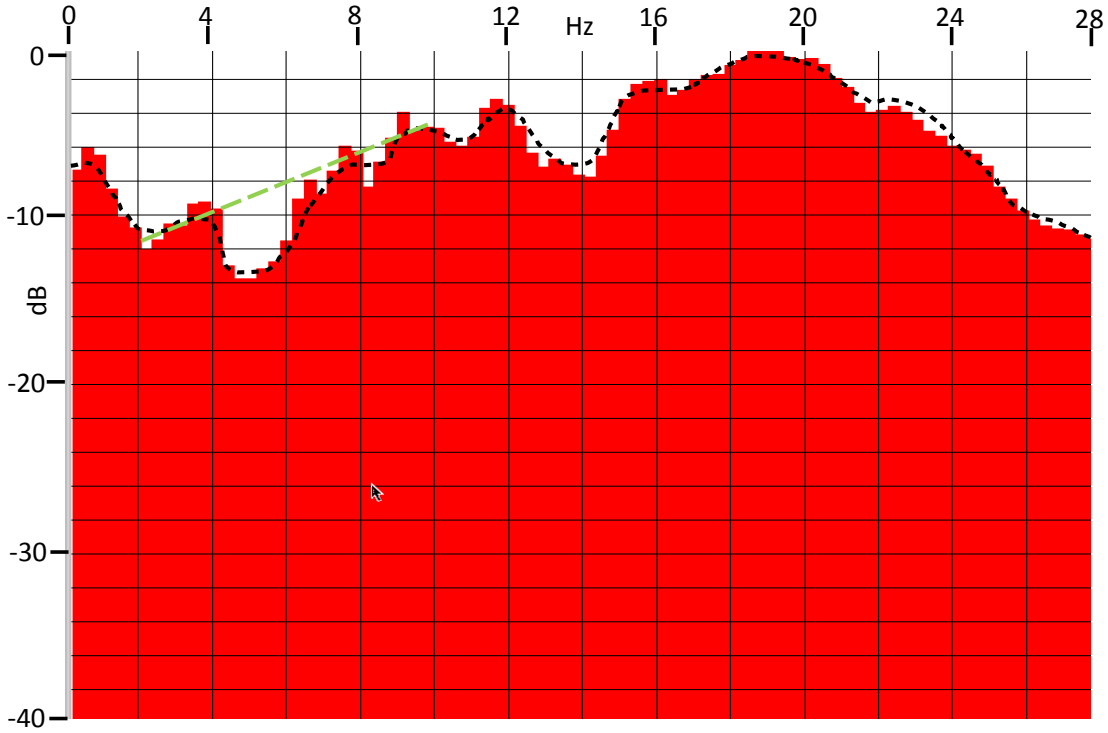

FIG.27. Low-frequency spectrum of dynamite source gather after subtraction of coherent noise. 2Hz-10Hz roll-off is much less than for 4.5Hz geophones. Low-frequency 'drift' component still present.

The Eagle Failing shot record into the Vectorseis spread is shown in Figure 28. As in the previous comparison, reflections are much weaker than on the dynamite data, and integration 'drift' fluctuations are evident on the traces. The coherent noise estimate appears in Figure 29, and the shot after filtering in Figure 30. The corresponding low-frequency spectra are featured in Figures 31, 32, and 33, respectively. It is interesting to note that on the spectrum of the filtered shot (Figure 33), the strong peak at about 1.5Hz probably represents 'drift' noise, which is now comparable in strength to the reflection signal itself.

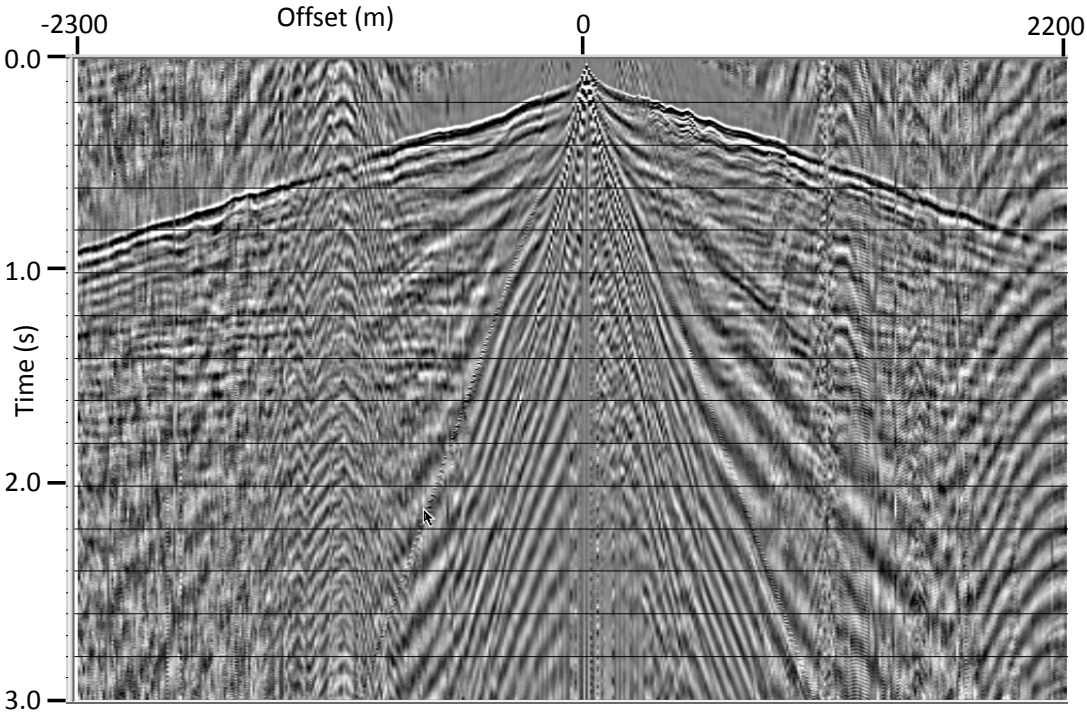

FIG.28. Source gather for EagleFailing y2400 recorded into vertical component of Vectorseis spread. Reflections are barely visible compared to coherent noise and stationary noise.

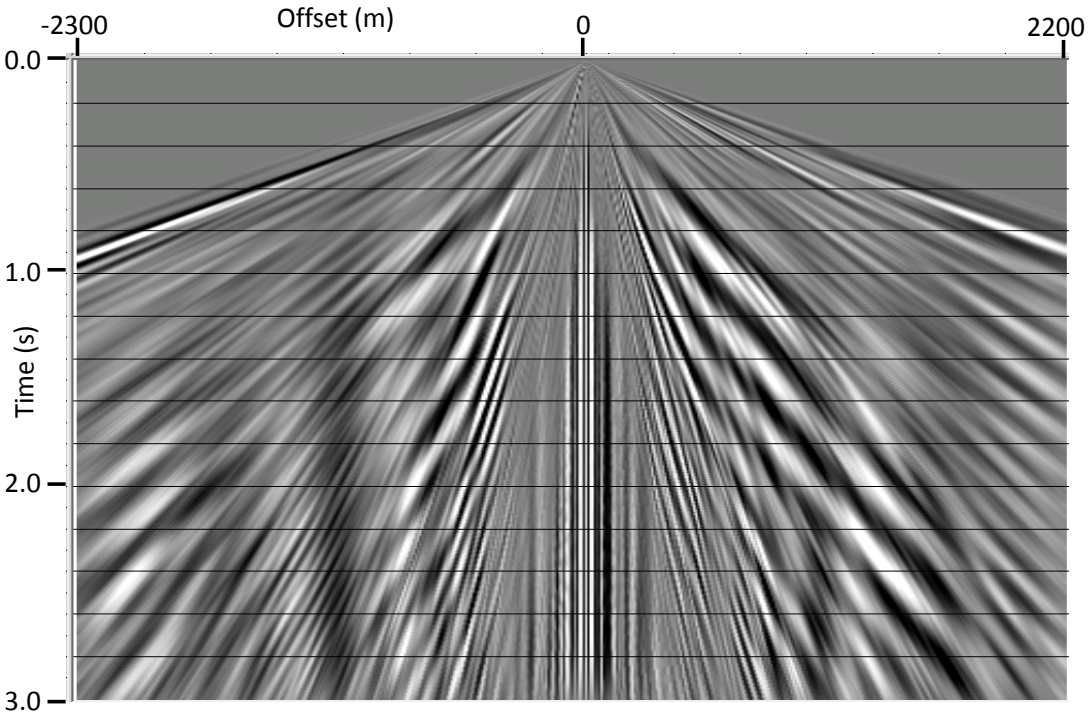

FIG.29. Most significant component of coherent noise as estimated in the RT domain.

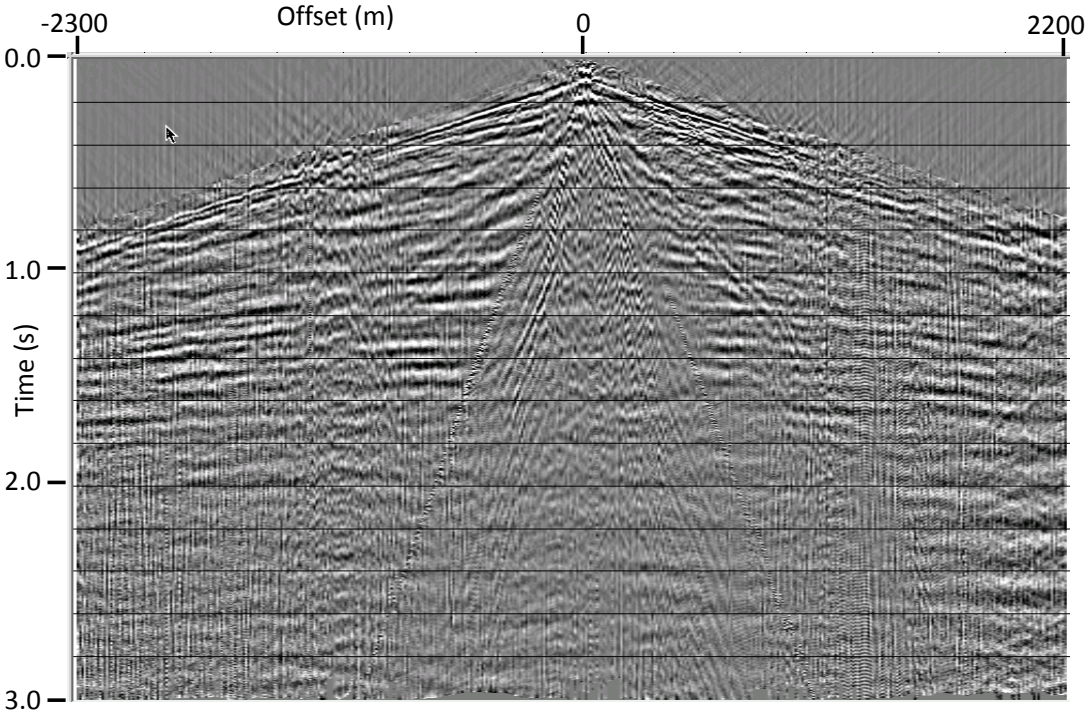

FIG.30. y2400 source gather after subtraction of coherent noise. Reflections are more visible, but still weak compared to residual coherent noise and ‘drift’ noise.

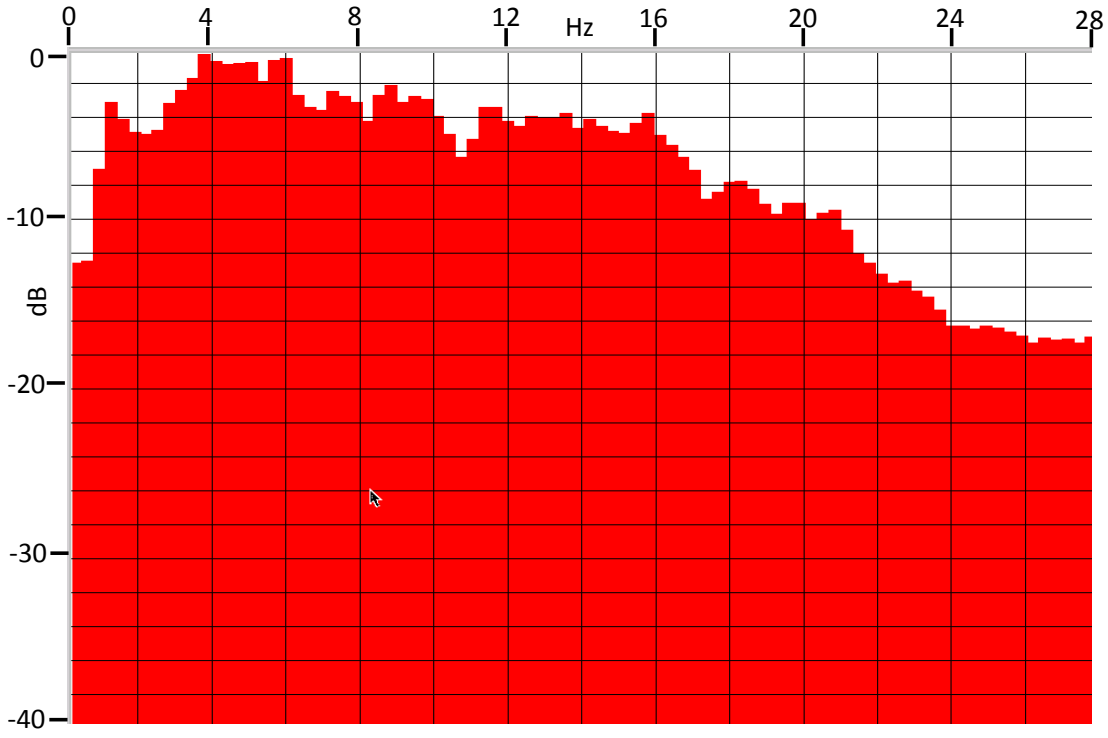

FIG.31. Low-frequency spectrum of y2400 source gather in Figure 28.

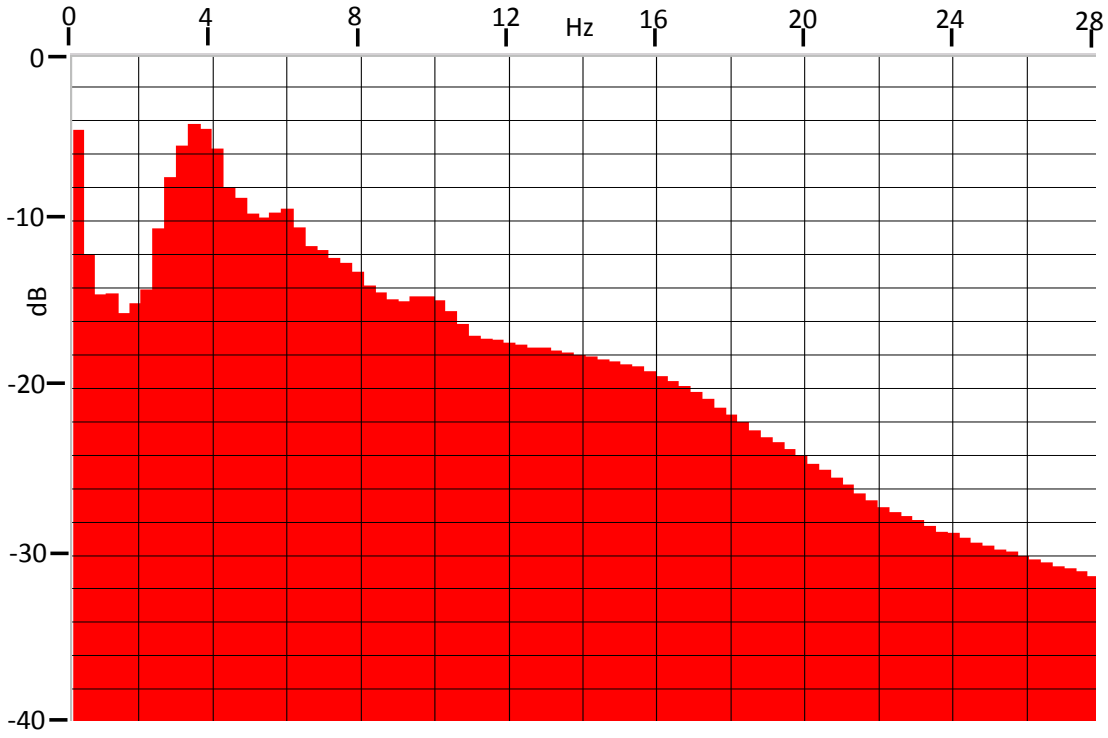

FIG.32. Low-frequency spectrum of coherent noise estimate in Figure 29.

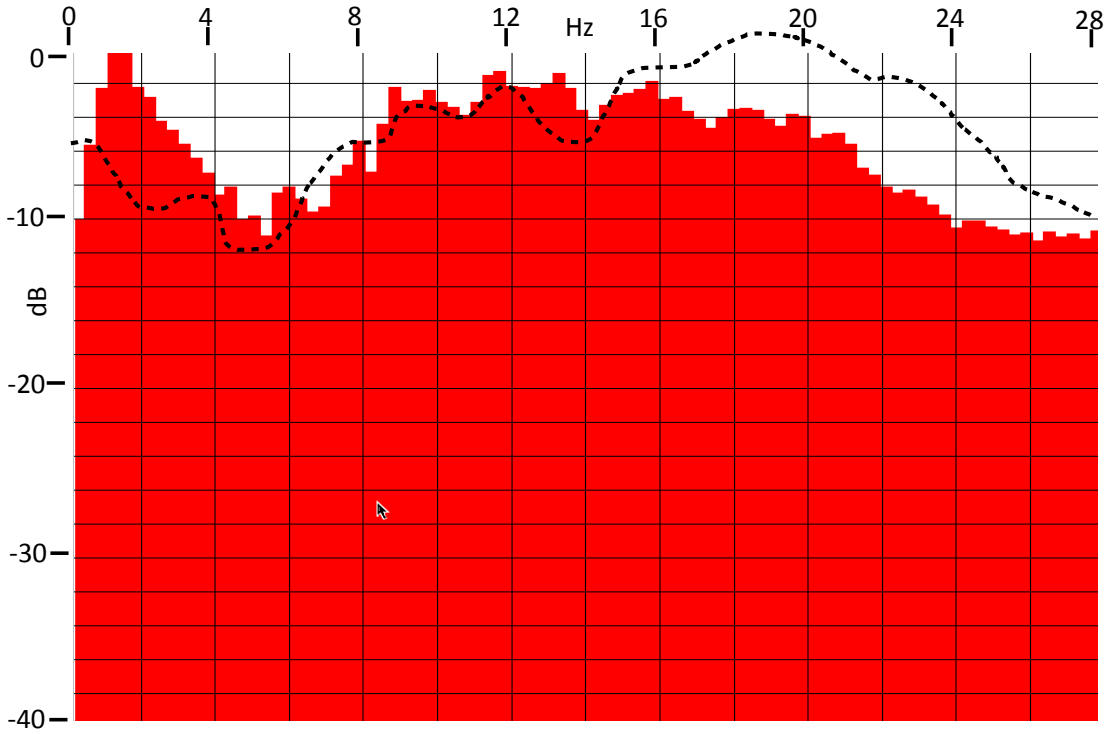

FIG.33. Low-frequency spectrum for y2400 source gather after subtraction of coherent noise. Dynamite spectrum superimposed for comparison. Note the survival of much more noise below 2Hz.

For the INOVA vibrator, the results are similar. The source gather, coherent noise estimate, and filtered source gather are shown in Figures 34, 35, and 36, respectively; and their respective low-frequency spectra constitute Figures 37, 38, and 39. As in the 4.5Hz spread comparison, the reflections are marginally stronger on the INOVA gather, both before and after noise attenuation, than on the Eagle Failing gather. Like the Eagle Failing result above, the low-frequency spectrum (Figure 39) of the INOVA noise-attenuated shot features a strong peak at 1.5Hz that is probably the manifestation of the integration 'drift' noise. In this figure, the peak is somewhat weaker than the peak of the seismic spectrum, while on the Eagle Failing result, the peak is somewhat stronger (Figure 33).

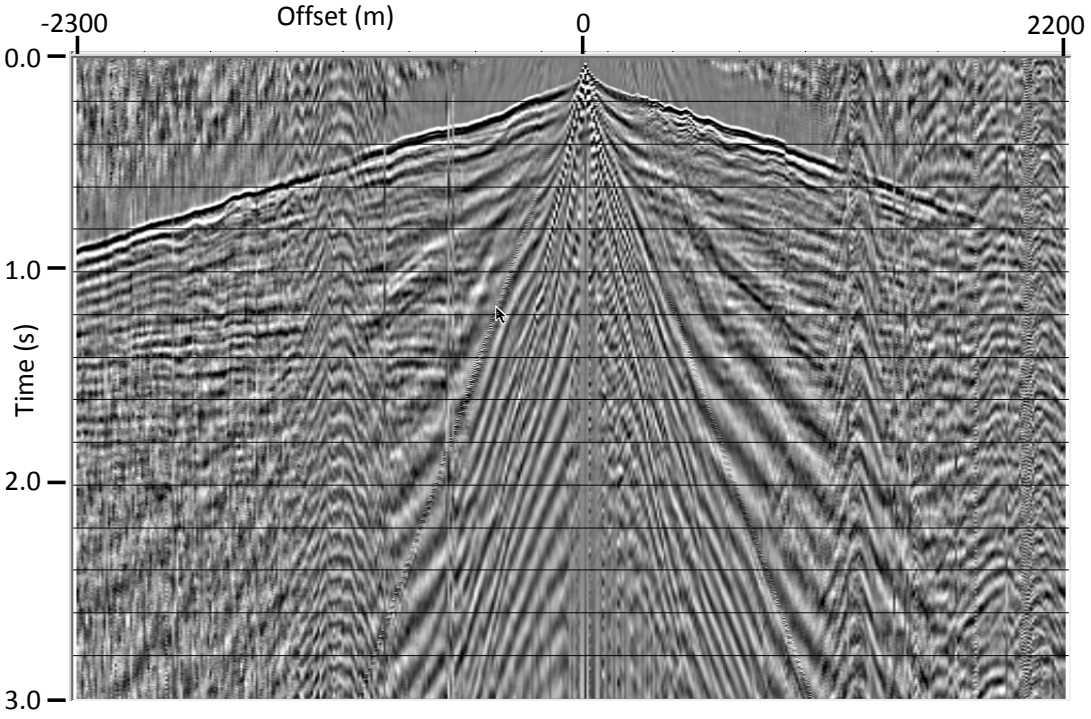

FIG.34. Source gather for INOVA Low-dwell vibrator as recorded on vertical component Vectorseis spread. Reflections very weak compared to coherent and stationary noise.

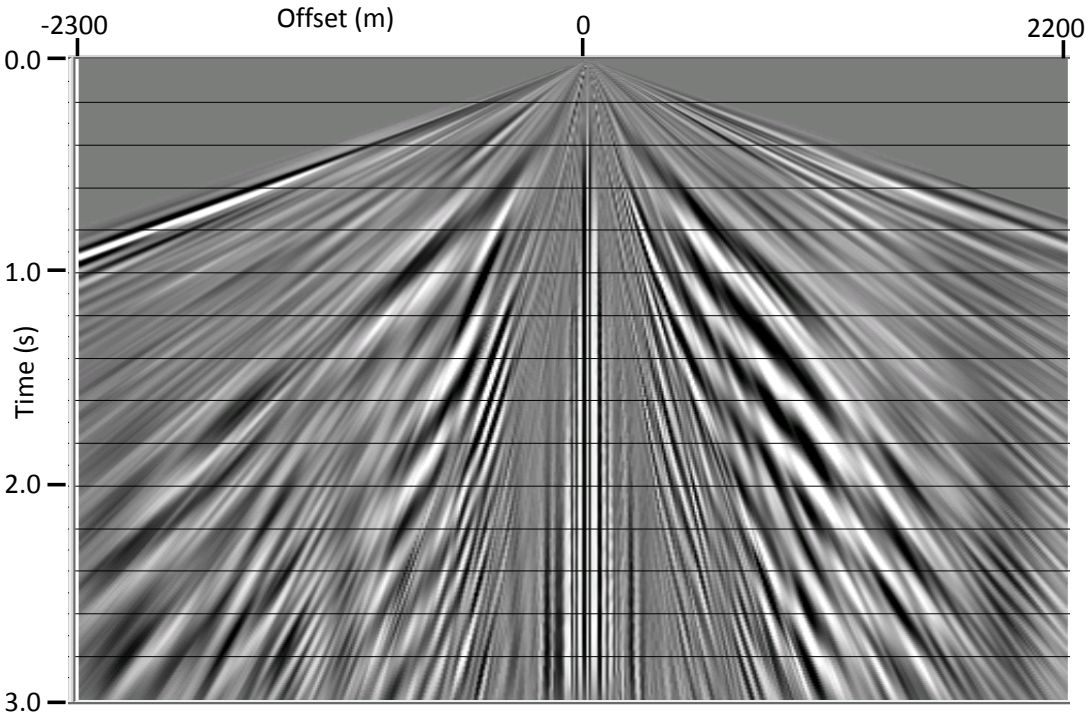

FIG.35. Most significant coherent noise component as estimated in teh RT domain.

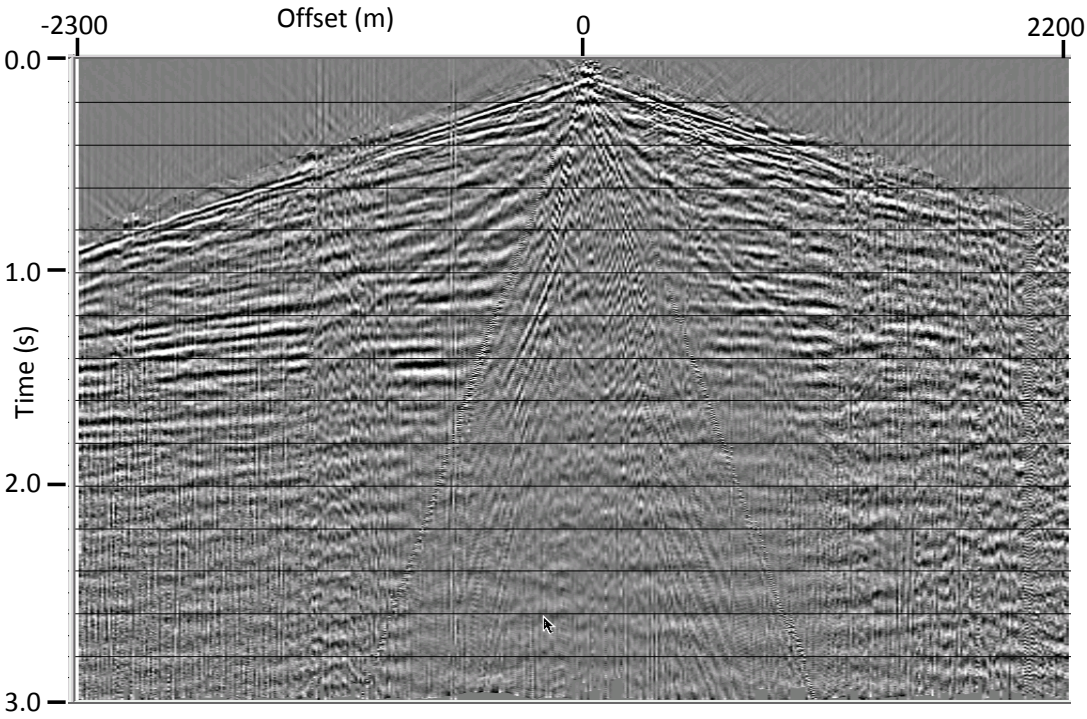

FIG.36. INOVA source gather after subtraction of coherent noise.

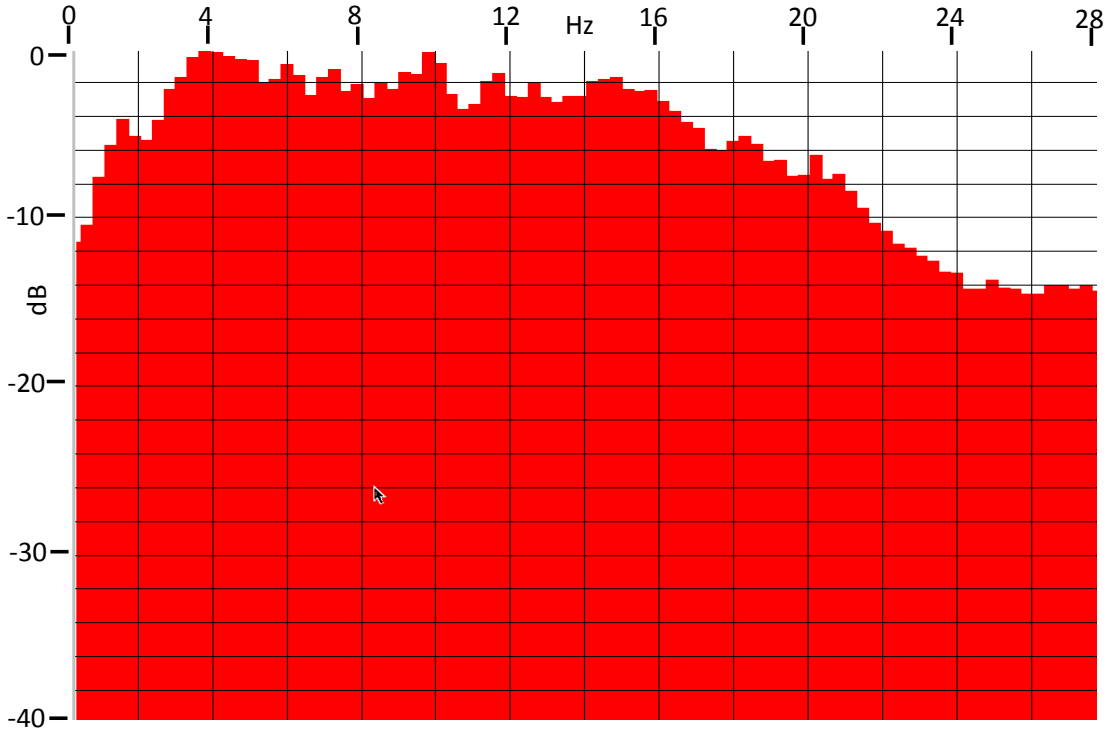

FIG.37. Low-frequency spectrum of raw INOVA source gather.

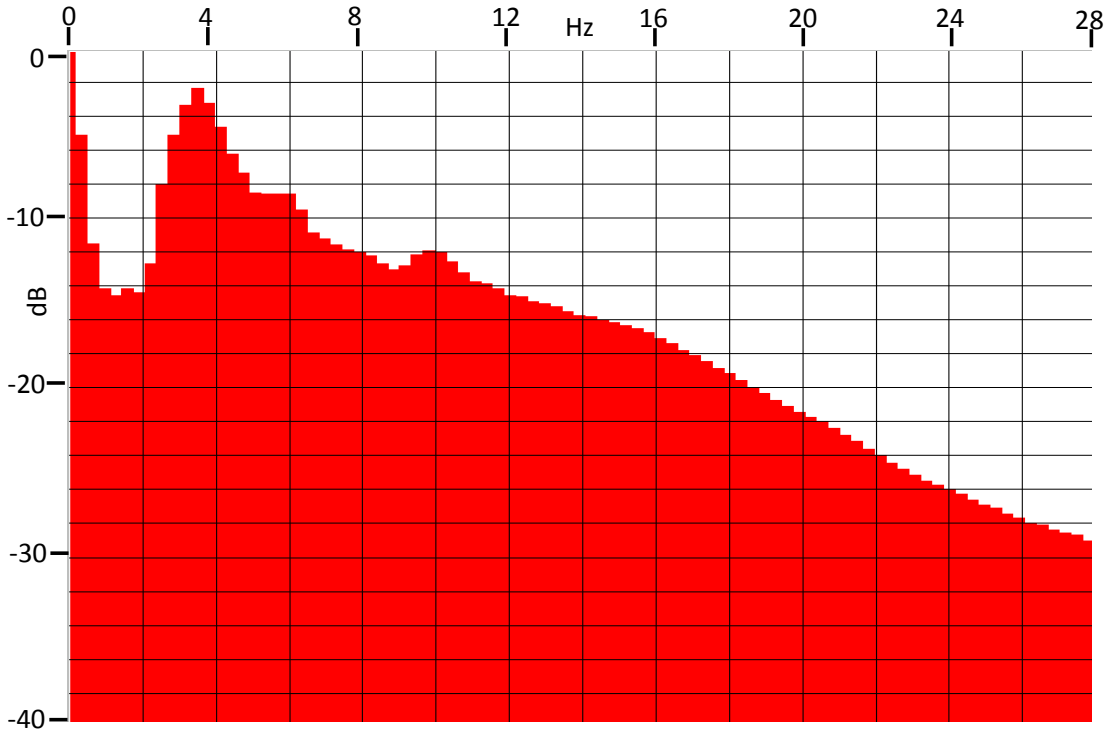

FIG.38. Low-frequency spectrum of coherent noise estimate in Figure 35.

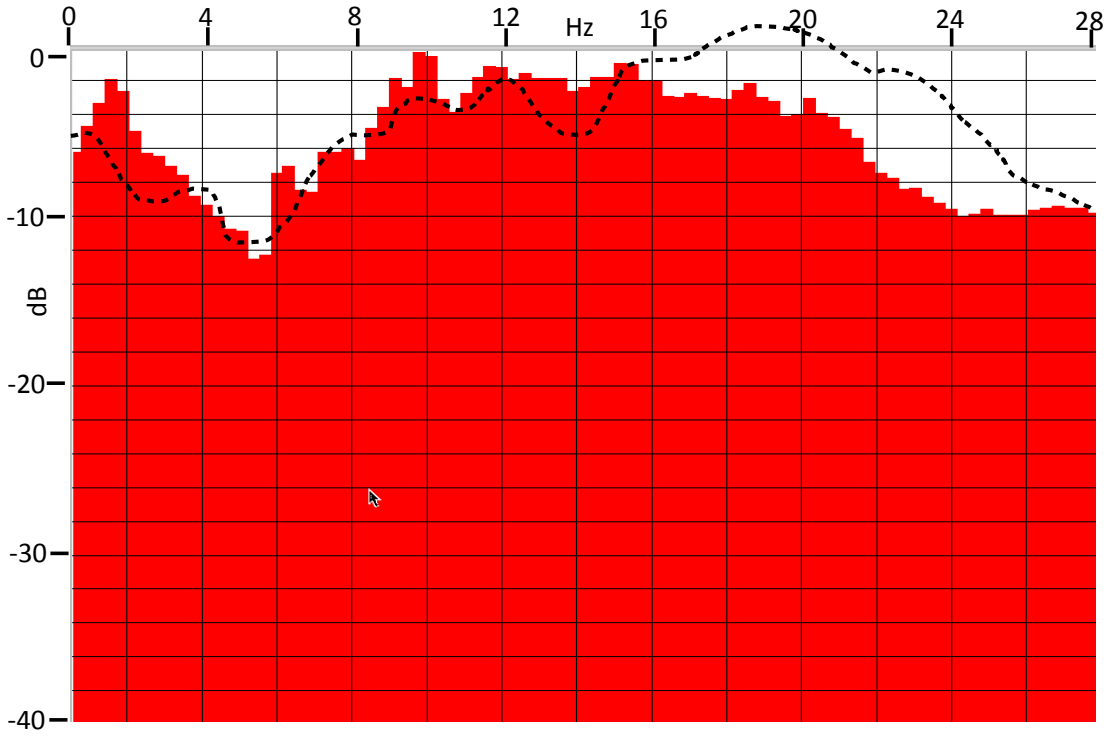

FIG.39. Low-frequency spectrum of INOVA source gather after coherent noise subtracted. Dynamite spectrum superimposed for comparison.

Further examination of Figure 27, the low-frequency spectrum of the dynamite shot, shows that on the Vectorseis spread, the spectral roll-off from 10Hz to 2Hz is only about 7dB, compared to 14dB on the 4.5Hz spread data (Figure 9). Because of the presence of the strong 'drift' component for the two Vibroseis sources, the spectral roll-off for these two sources can't be reliably estimated.

THE ULTIMATE GOAL

Although we've been examining source-induced low-frequency reflection content on single source gathers, the ultimate goal is to create full seismic images with increased bandwidth, particularly on the low-frequency end. As an example of where this might lead, in another project (Henley, 2012b), we have processed both the vertical and radial components of the dynamite Vectorseis data, from raw records to static-corrected stacked section, with the aim of bandwidth preservation. The processing stages included RT filtering, pre-stack Gabor deconvolution, raypath interferometry (Henley, 2012a) for statics, CMP stacking, post-stack Gabor deconvolution (spectral whitening), and FX deconvolution (random noise attenuation). Figure 40 shows the processed section for the vertical component, and Figure 41 its average power spectrum. The spectral roll-off below about 4Hz is primarily a result of filter application, and probably doesn't reflect the true spectral content of the underlying reflections, which may be as low as 2Hz.

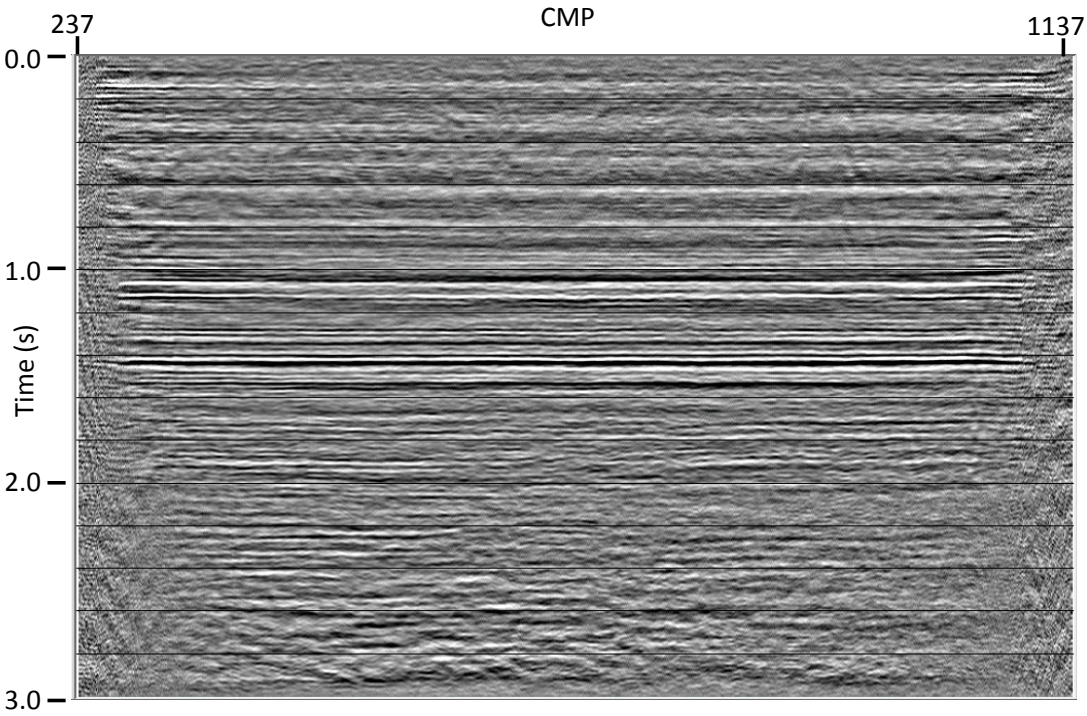

FIG.40. Stacked section from Vectorseis vertical component dynamite shots. Gabor deconvolution has been applied pre-stack and post-stack, raypath interferometry has been used to apply static corrections.

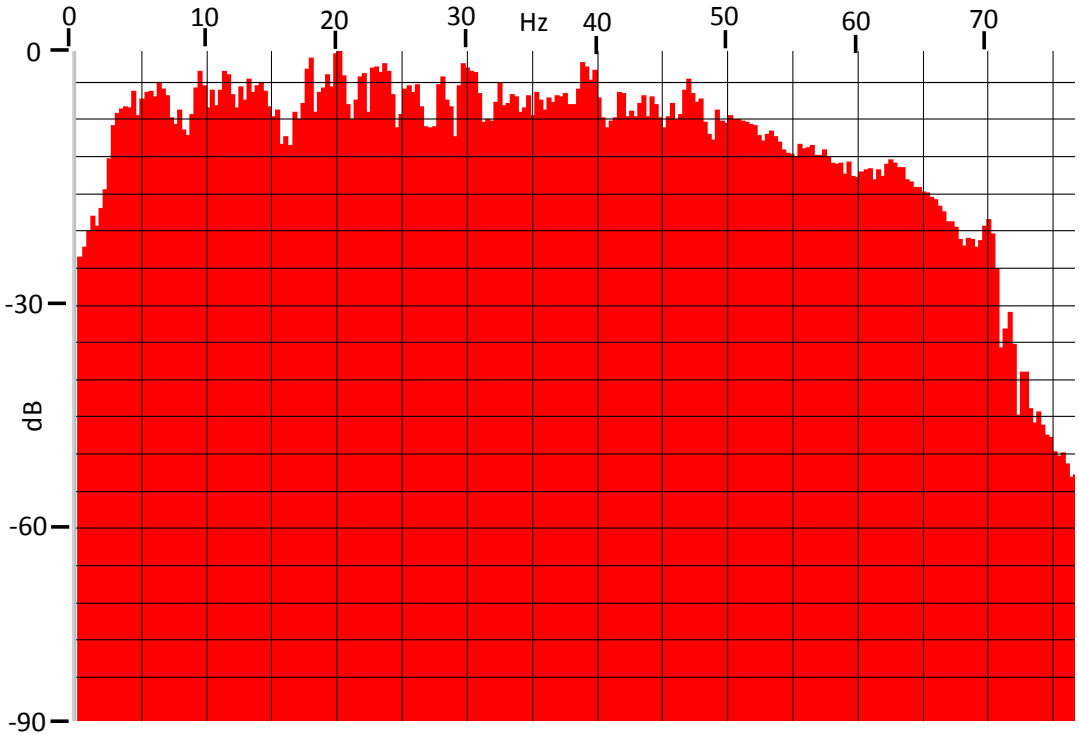

FIG.41. Spectrum of stack image shown in Figure 40. Significant bandwidth of the image is approximately 2Hz-55Hz, between the -10dB points on the high- and low-end roll-off.

CONCLUSIONS

The reflections recorded with a dynamite source, both into the 4.5Hz geophone spread and the Vectorseis accelerometer spread, were significantly stronger relative to surface wave noise than those recorded using either the Failing Eagle y2400 vibrator, or the INOVA 364 vibrator, although both used specially designed low-dwell sweeps of 1-100Hz. Furthermore, the dynamite data displayed a somewhat higher dominant frequency, at 20Hz, compared to 14Hz for the Vibroseis (in the absence of any spectral whitening). After noise removal, data from all three sources exhibited similar low-frequency spectral roll-off on the 4.5Hz phones, probably controlled by the geophone characteristics. On the Vectorseis data, the dynamite data appeared to have coherent frequencies down to about 2Hz, while both sets of Vibroseis data were more affected by integration 'drift' noise in that portion of the spectrum (probably due to weaker reflection signal overall). Although at this particular source point, the INOVA vibrator appeared slightly stronger in usable reflection strength, at other source points, the Eagle Failing vibrator was slightly better.

ACKNOWLEDGEMENTS

The author thanks all parties participating in the Hussar experiment for access to the data, and CREWES staff, especially Helen Isaac, for preliminary processing. He also thanks CREWES sponsors and NSERC for continuing financial support of the project.

REFERENCES

Henley, D.C., 2003, Coherent noise attenuation in the radial trace domain, Geophysics, **68**, No. 4, (JulyAug 2003), pp1408-1416.

Henley, D.C., 2011, Now you see it, now you don't: radial trace filtering tutorial, 2011 CREWES research report, **23.**

Henley, D.C., 2012a, Interferometric application of static corrections, Geophysics, **77,** No. 1 (Jan-Feb 2012), PQ1-Q13

Henley, D.C., 2012b, Interference and the art of static corrections: raypath interferometry at Hussar, 2012 CREWES research report, **24.**

Isaac, J.H., and Margrave, G.F., 2011, Hurrah for Hussar! Comparisons of stacked data, 2011 CREWES research report, **23.**

Lloyd, H.J.E., and Margrave, G.F., 2011, Comparison of low frequency data of geophones to well logs - Hussar example, 2011 CREWES research report, **23.**

Margrave, G.F., Mewhort, L., Phillips, T., Hall, M., Bertram, M.B., Lawton, D.C., Innanen, K.A.H., Hall, K.W., and Bertram, K., 2011, The Hussar low-frequency experiment, 2011 CREWES research report, **23**.